

Workshop on Nuclear Resonant Scattering and Data Analysis
November 11 – 13, Advanced Photon Source

Studies of Thin-Film Magnetism Using Nuclear Resonant Scattering

Ralf Röhlsberger

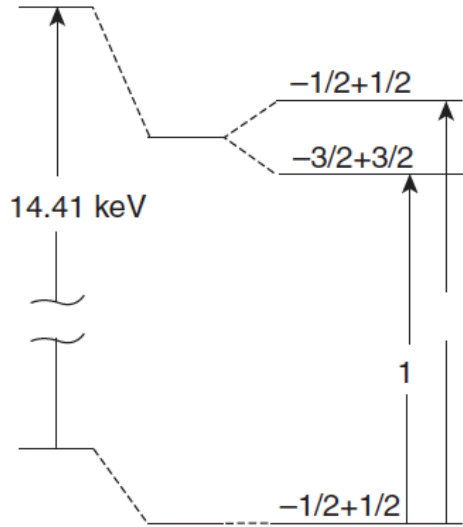
Deutsches Elektronen-Synchrotron DESY, Hamburg

Outline

- 1. Hyperfine Interactions:
Mössbauer nuclei as spectators of solid-state properties**
- 2. Magnetic structure of thin films, multilayers and nanostripes**
 - a. Spin structure of exchange-spring magnets
 - b. Domain-wall compression at magnetic interfaces
 - c. Twisted magnetic structures in multilayers
 - d. Magnetic order in nanostripe arrays
- 3. Magnetic dynamics in thin films and nanostructures**
 - a. Superparamagnetic relaxation in nanoparticles
 - b. Spin precession at ferromagnetic resonance

Hyperfine Interactions

Electric hyperfine interaction

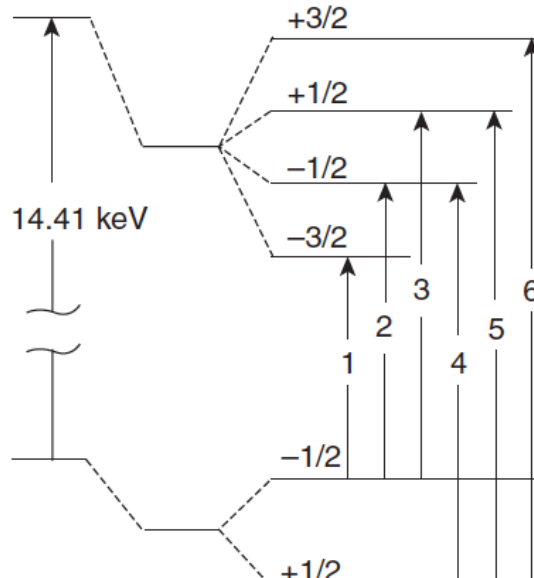


Isolated nucleus Isomer shift Electric field gradient

$$\Delta E_q = \frac{\pm 1}{4} e Q V_{zz} \left(1 + \frac{\eta^2}{3} \right)^{1/2}$$

$$\eta \equiv (V_{xx} - V_{yy}) / V_{zz}.$$

Magnetic hyperfine interaction

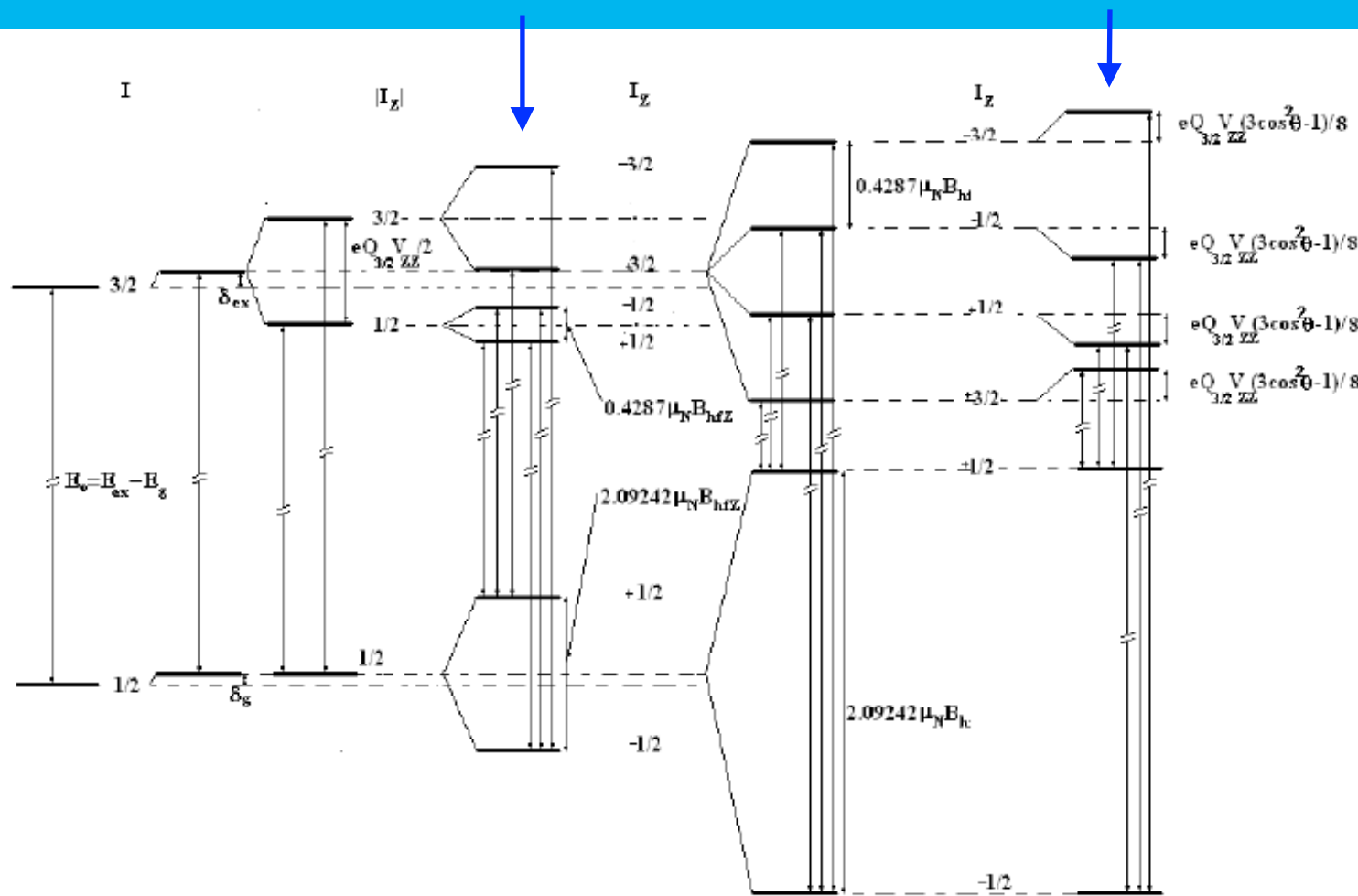


Isolated nucleus Isomer shift Hyperfine magnetic field

$$\Delta E_m = (m_e g_e - m_g g_g) B$$

From: Brent Fultz, in: 'Characterization of Materials', Wiley 2012

Combined Hyperfine Interaction: Electric + Magnetic



$$V_{zz}=0; B_{hf}=0$$

$$V_{zz}\neq 0; B_{hf}=0$$

$$V_{zz}=0; B_{hf}\neq 0$$

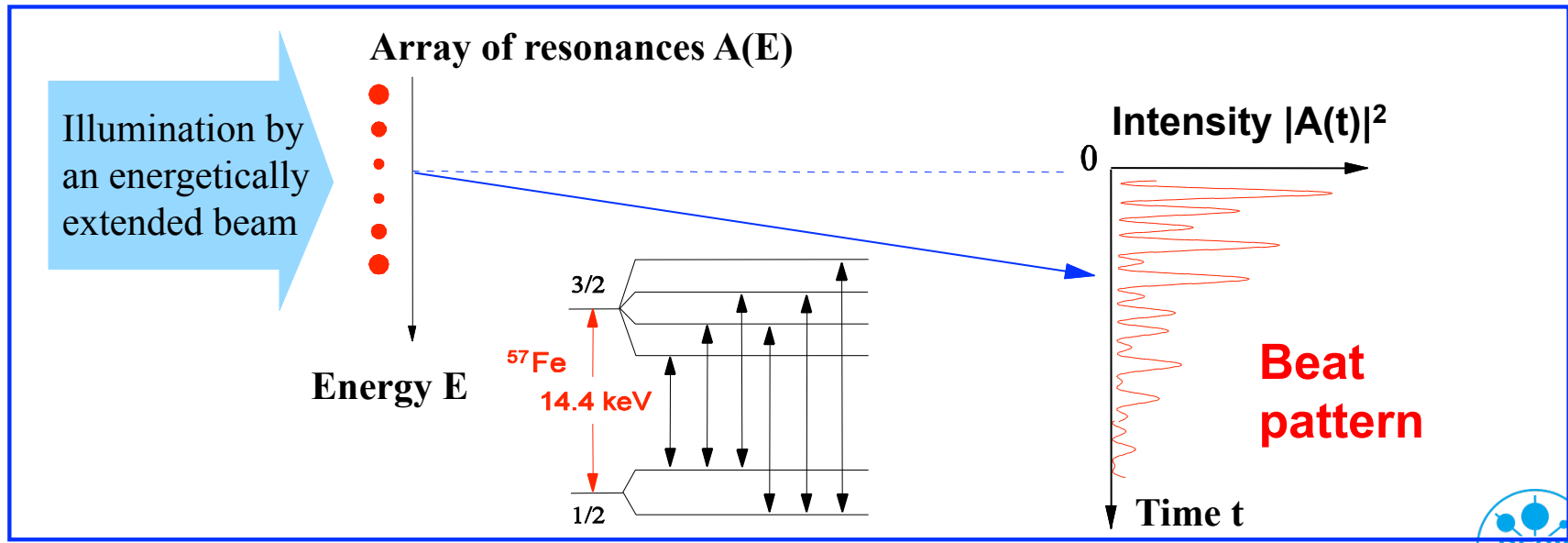
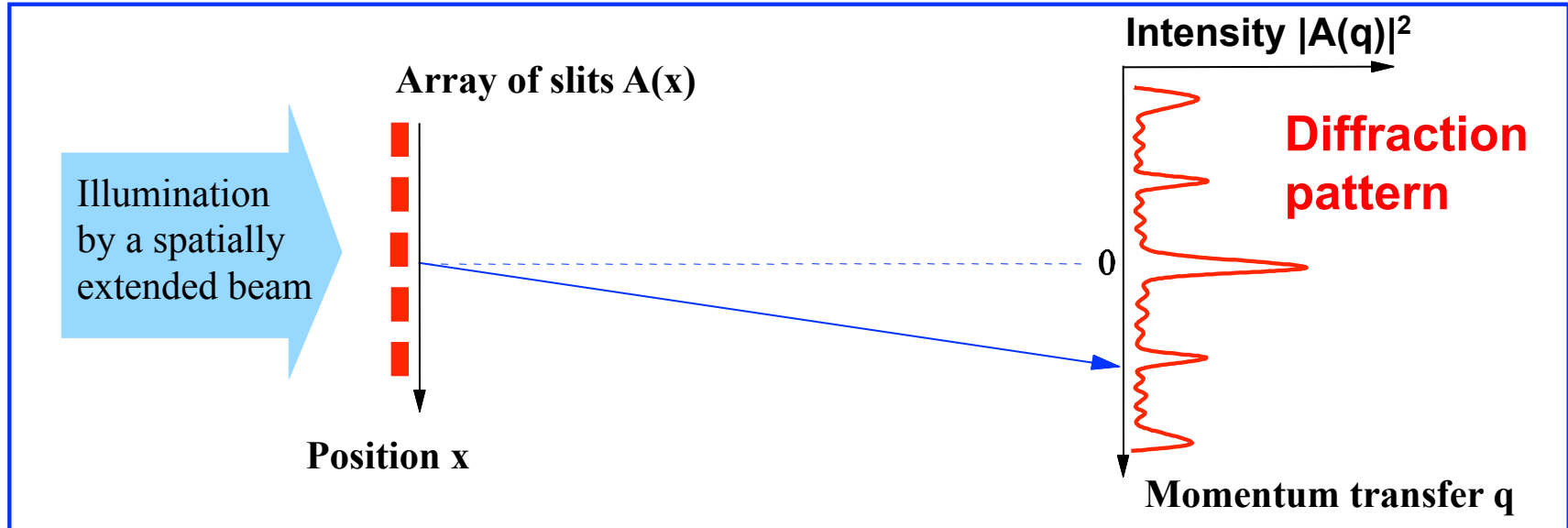
$$\mu_N B_{hf} \ll eQ_{3/2}V_{zz}/2$$

$$V_{zz}=0; B_{hf}\neq 0$$

$$V_{zz}\neq 0; B_{hf}=0$$

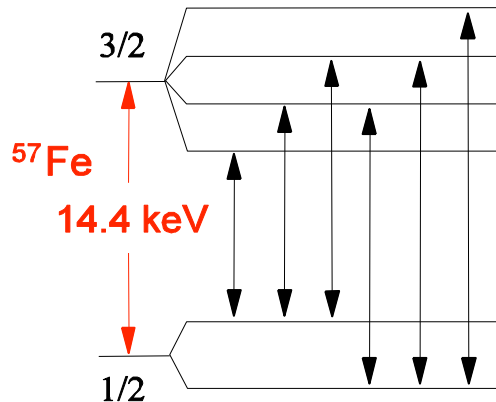
$$\mu_N B_{hf} \gg eQ_{3/2}V_{zz}/2$$

Diffraction as Method of Structure Determination



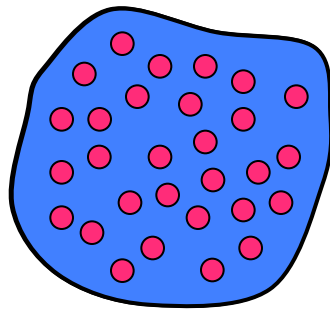
Nuclear Resonant Forward Scattering of Synchrotron Radiation

Pulsed broadband excitation of hyperfine-split nuclear levels



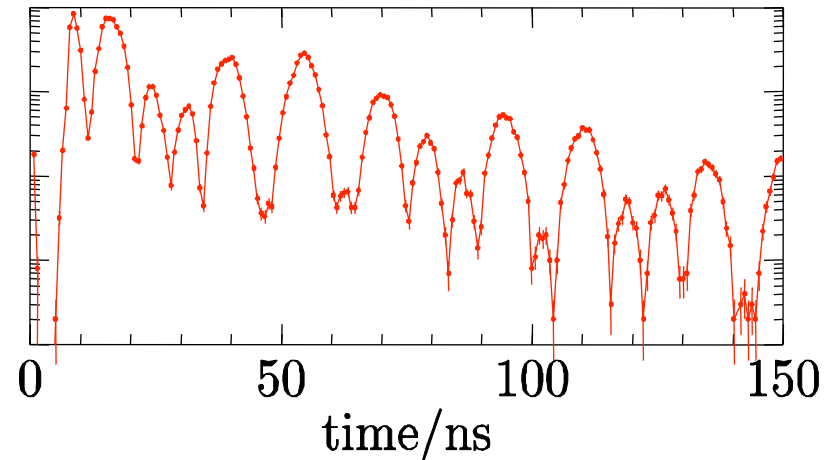
The 14.4 keV nuclear resonance of ^{57}Fe

$$\tau_0 = 141 \text{ ns}, \Gamma_0 = 4.7 \text{ neV}$$



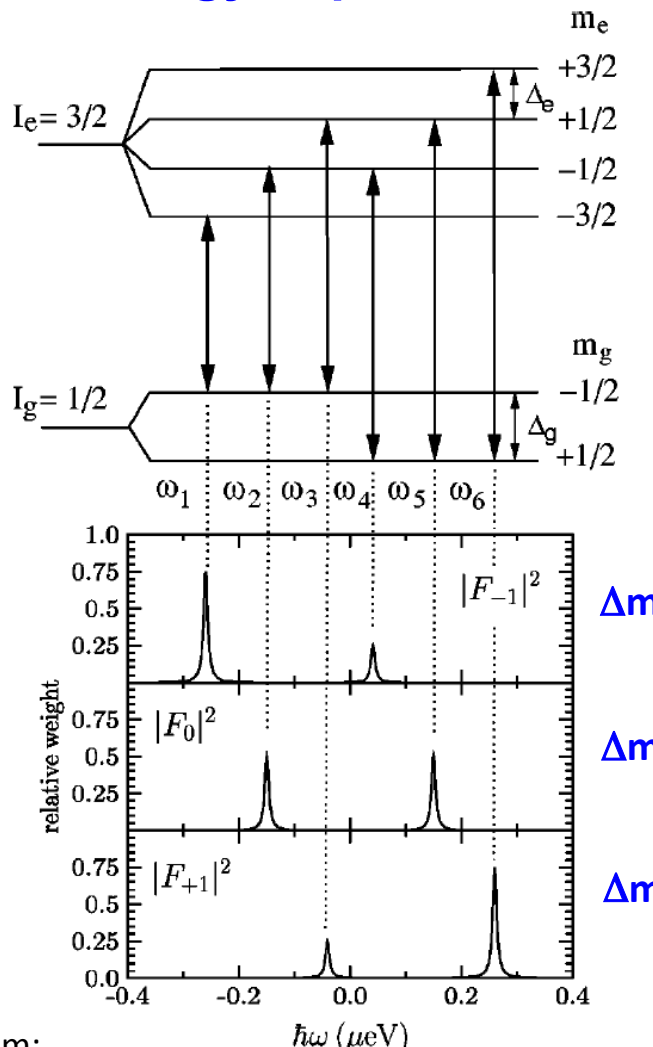
The beat pattern is a fingerprint of the magnetic structure of the sample:

Temporal beats



Magnetic Hyperfine Interaction

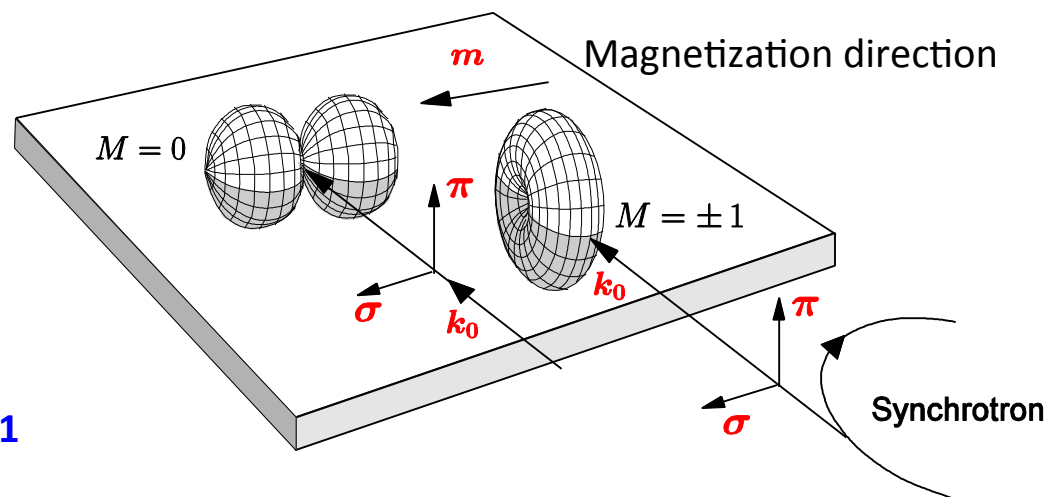
Energy dependence



From:

Phys. Rev. B 67, 245412 (2003)

Directional dependence → Dipole emission characteristics



$\Delta m = -1$

$\Delta m = 0$

$\Delta m = +1$

Magnetic Hyperfine Interaction

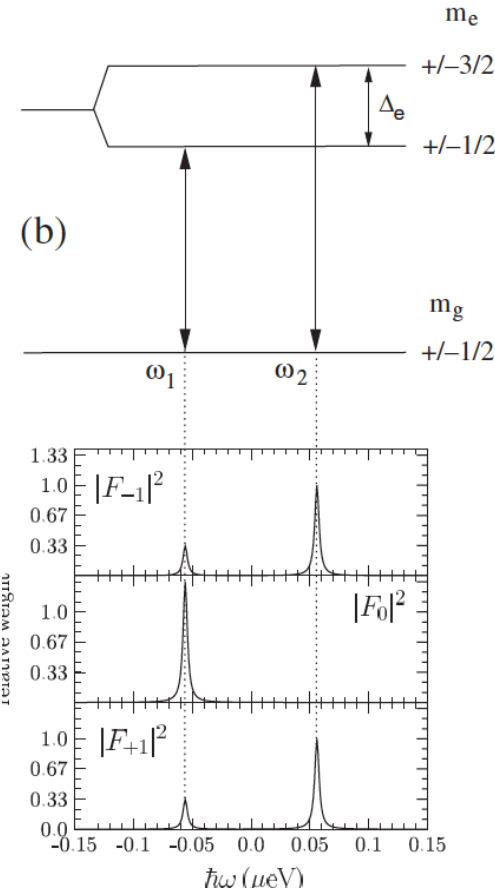
Directional dependence

	Geometry	Nuclear Scattering Length $N(\omega)$	Time spectrum $\sigma \rightarrow \text{unpolarized}$
A		$\frac{3}{16\pi} \begin{pmatrix} F_{+1} + F_{-1} & -i(F_{+1} - F_{-1}) \\ i(F_{+1} - F_{-1}) & F_{+1} + F_{-1} \end{pmatrix}$	
B		$\frac{3}{16\pi} \begin{pmatrix} F_{+1} + F_{-1} & 0 \\ 0 & 2F_0 \end{pmatrix}$	
C		$\frac{3}{16\pi} \begin{pmatrix} 2F_0 & 0 \\ 0 & F_{+1} + F_{-1} \end{pmatrix}$	
D		$\frac{3}{16\pi} \begin{pmatrix} F_{+1} + F_{-1} & 0 \\ 0 & F_{+1} + F_{-1} \end{pmatrix}$	
E		$f_{\sigma\sigma} = f_{\pi\pi} = \frac{3}{32\pi} (F_{+1} + F_{-1} + 2F_0)$	
F		$f_{\sigma\sigma} = \frac{3}{16\pi} (F_{+1} + F_{-1})$ $f_{\pi\pi} = \frac{3}{32\pi} (F_{+1} + F_{-1} + 2F_0)$	
G		$f_{\sigma\sigma} = f_{\pi\pi} = \frac{1}{8\pi} (F_{+1} + F_{-1} + F_0)$	

From:
Phys. Rev. B 67, 245412 (2003)

Electric Hyperfine Interaction

Directional dependence



	Geometry	Nuclear Scattering Length $N(\omega)$	Time spectrum $\sigma \rightarrow$ unpolarized
A		$\frac{3}{8\pi} \begin{pmatrix} F_{+1} & 0 \\ 0 & F_{+1} \end{pmatrix}$	
B		$\frac{3}{8\pi} \begin{pmatrix} F_{+1} & 0 \\ 0 & F_0 \end{pmatrix}$	
C		$\frac{3}{8\pi} \begin{pmatrix} F_0 & 0 \\ 0 & F_{+1} \end{pmatrix}$	
D		$\frac{3}{16\pi} \begin{pmatrix} F_0 + F_{+1} & F_0 - F_{+1} \\ F_0 - F_{+1} & F_0 + F_{+1} \end{pmatrix}$	
E		$f_{\sigma\sigma} = f_{\pi\pi} = \frac{3}{16\pi} (F_{+1} + F_0)$	
F		$f_{\sigma\sigma} = \frac{3}{8\pi} F_{+1}$ $f_{\pi\pi} = \frac{3}{16\pi} (F_{+1} + F_0)$	
G		$f_{\sigma\sigma} = f_{\pi\pi} = \frac{1}{8\pi} (2F_{+1} + F_0)$	

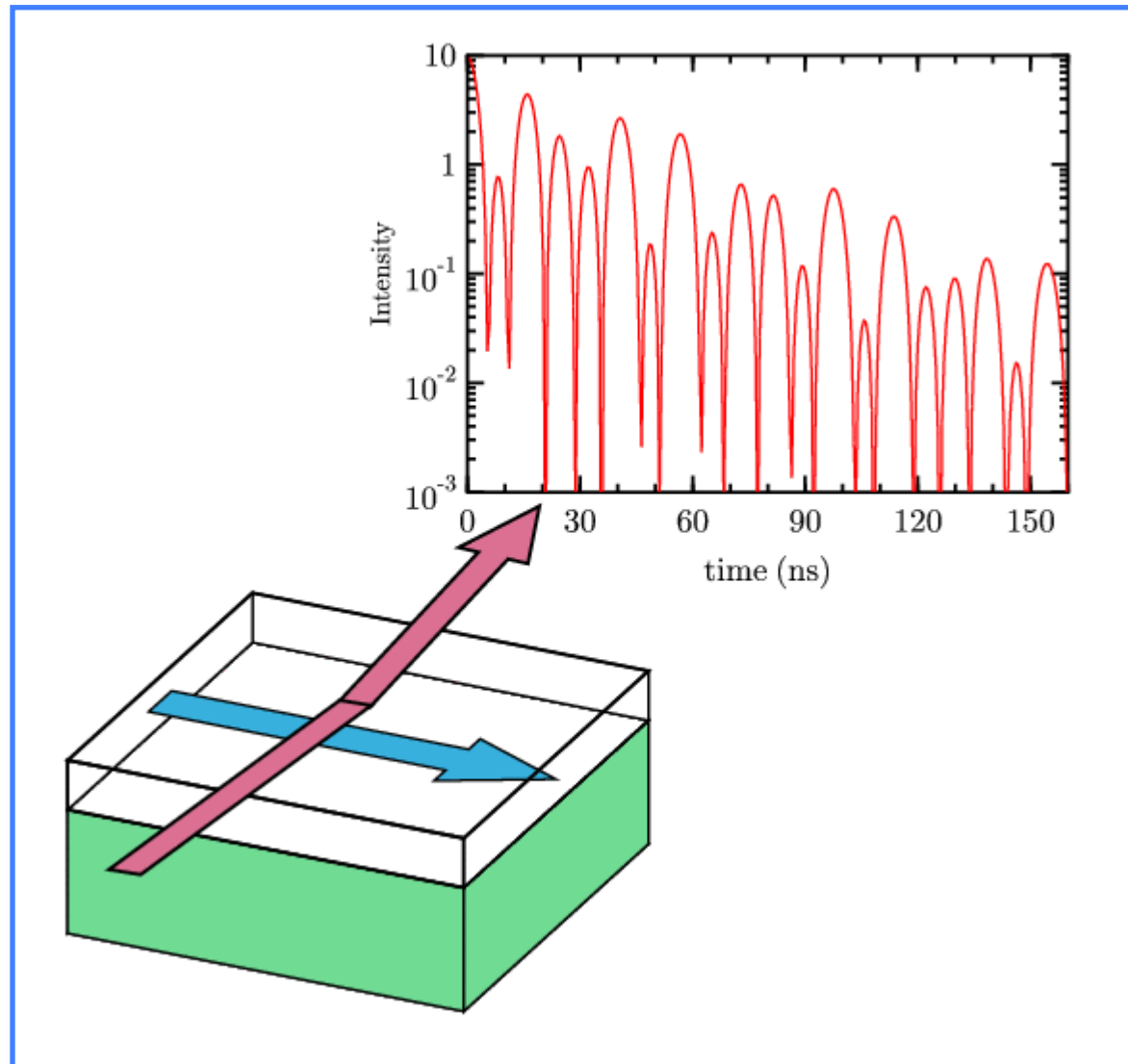
From:

R. Röhlsberger, Springer Tracts in Modern Physics, Vol. 208 (2005)

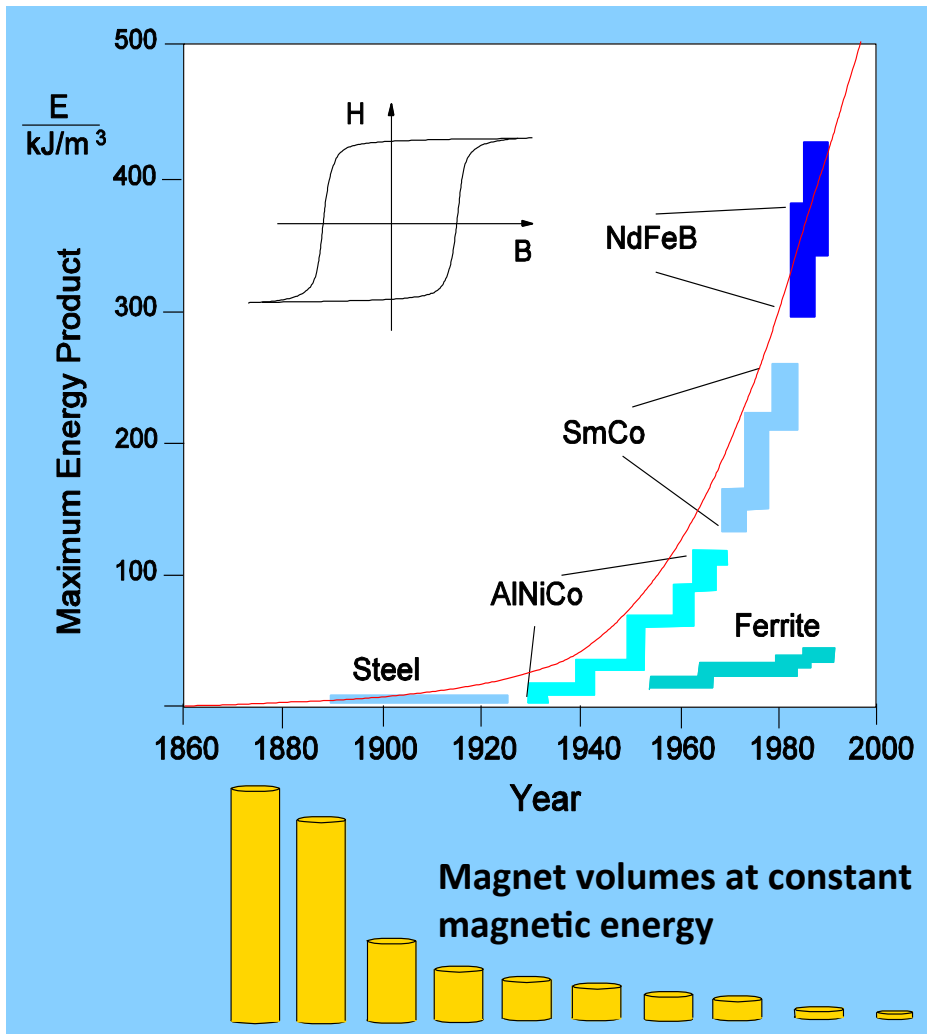
Temporal beats and magnetization direction

The temporal beat pattern sensitively depends on the orientation of the Magnetization M relative to the Photon wavevector k_0

→ Use isotopic probe layers to investigate the depth dependence of magnetic properties



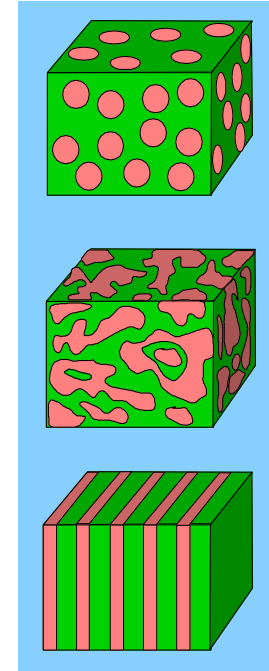
Permanent Magnets: Evolution of the Energy Product



Exchange hardening
in nanostructured
two-phase systems:

Hard phase with
high coercivity

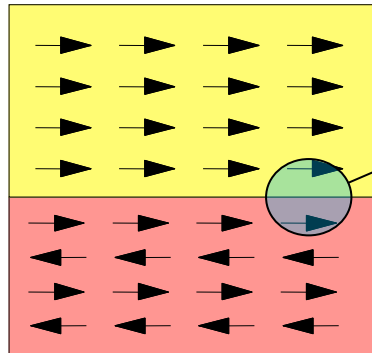
Soft phase with
high magnetization



R. Skomski and J. Coey:
PRB 48, 15812 (1993)

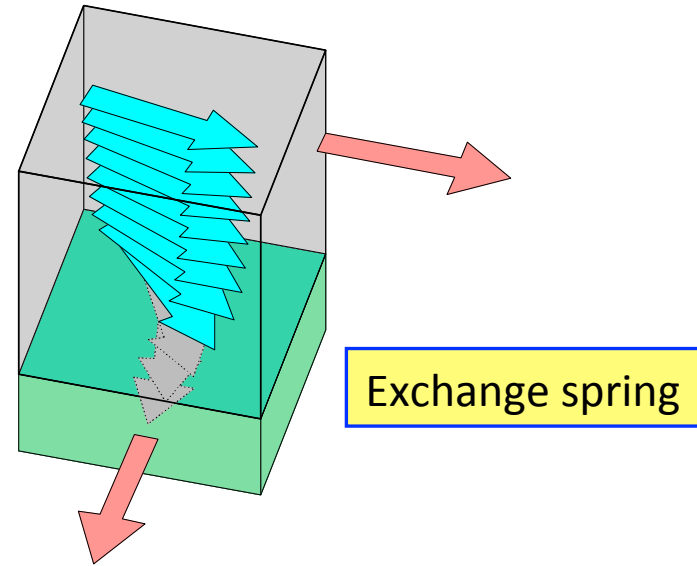
Exchange-Coupled Bilayers

Ferromagnet/Antiferromagnet

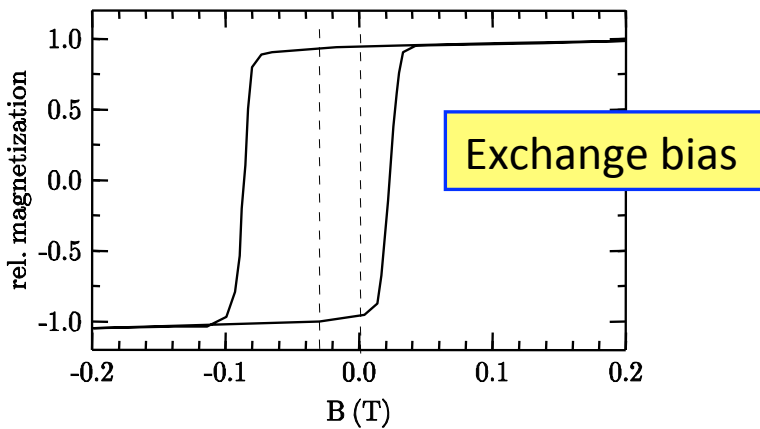


What happens at
the interface ?

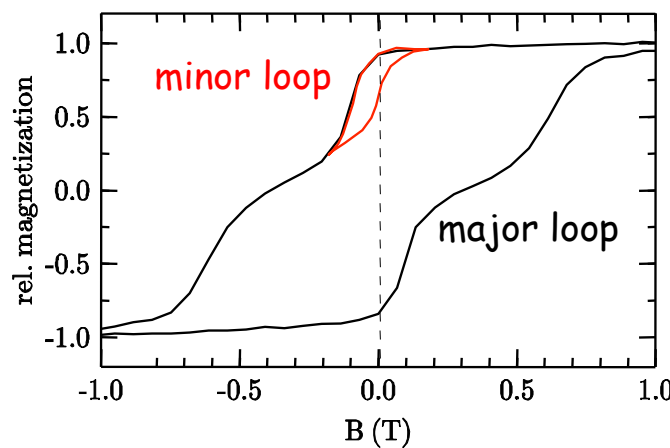
Hard magnet/Soft magnet



Magnetic hysteresis



Magnetic hysteresis



The Spin Structure of Magnetic Bilayers

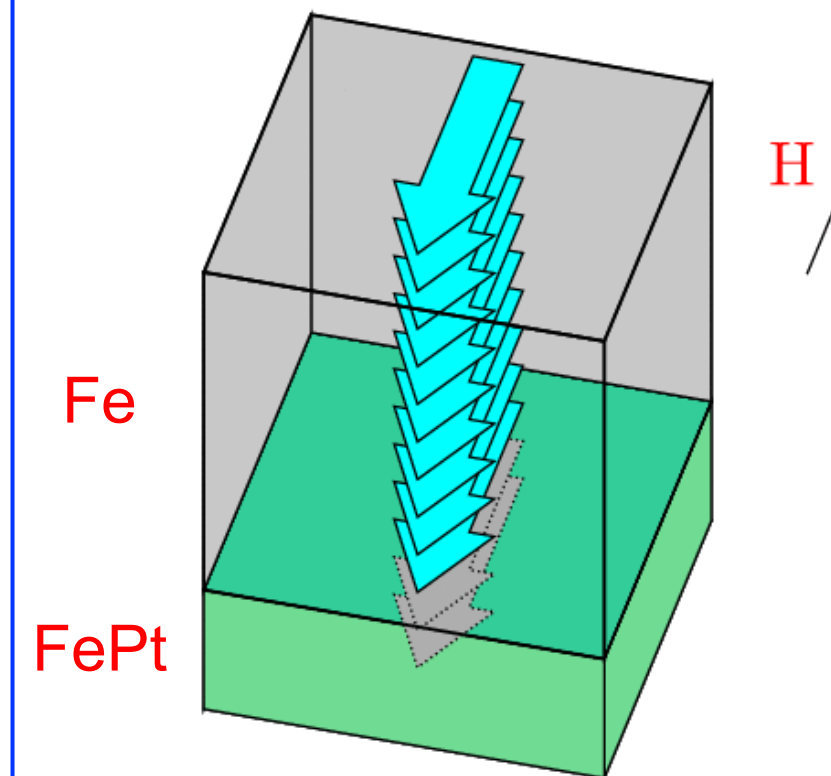
Fe on FePt

Soft – magnetic Fe

Hard – magnetic FePt
with uniaxial anisotropy

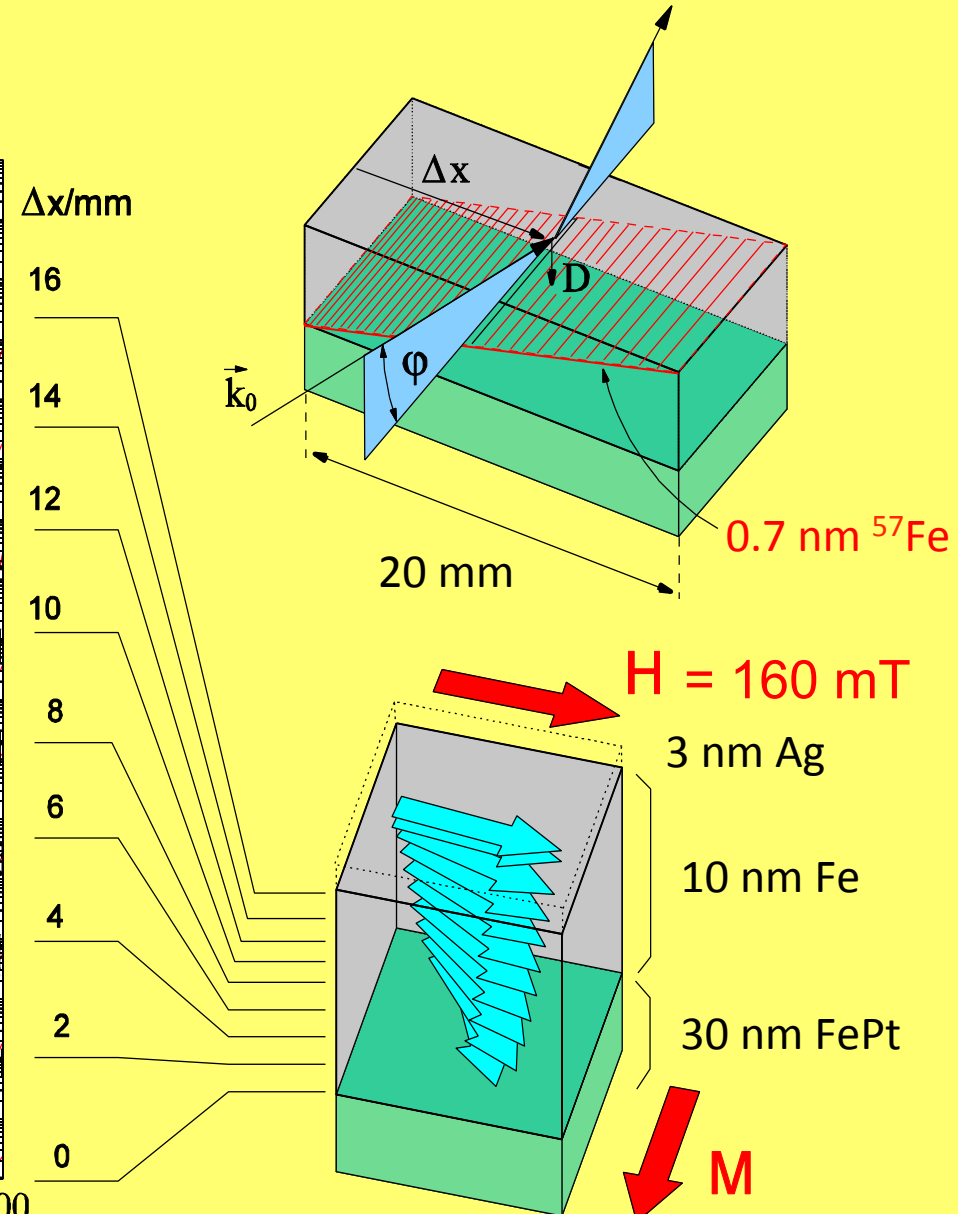
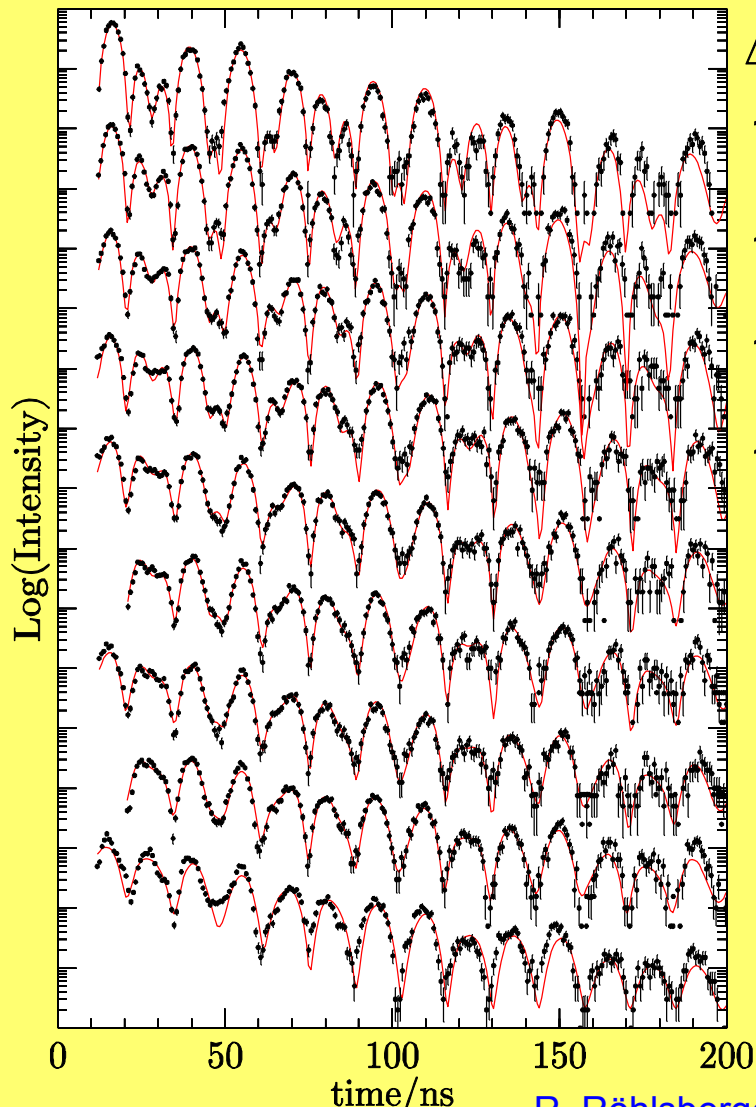
- Exchange coupling at the interface: Parallel alignment of Fe and FePt moments
- With increasing distance from the interface: Coupling becomes weaker
- External field H induces spiral magnetization
- Return to parallel alignment for $H = 0$

Exchange-Spring magnets

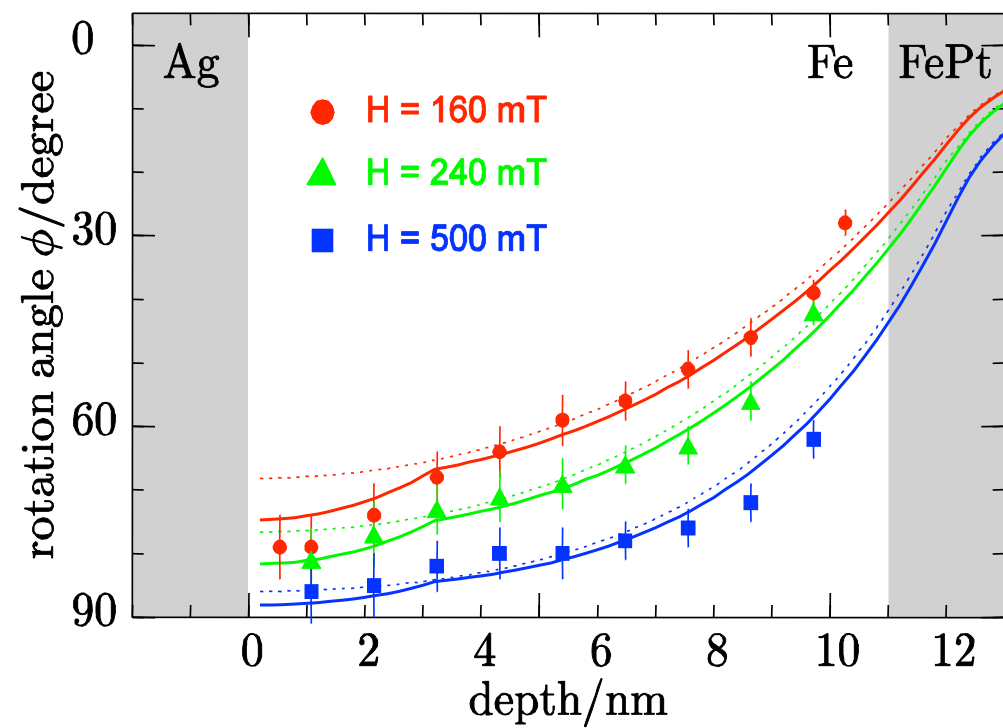
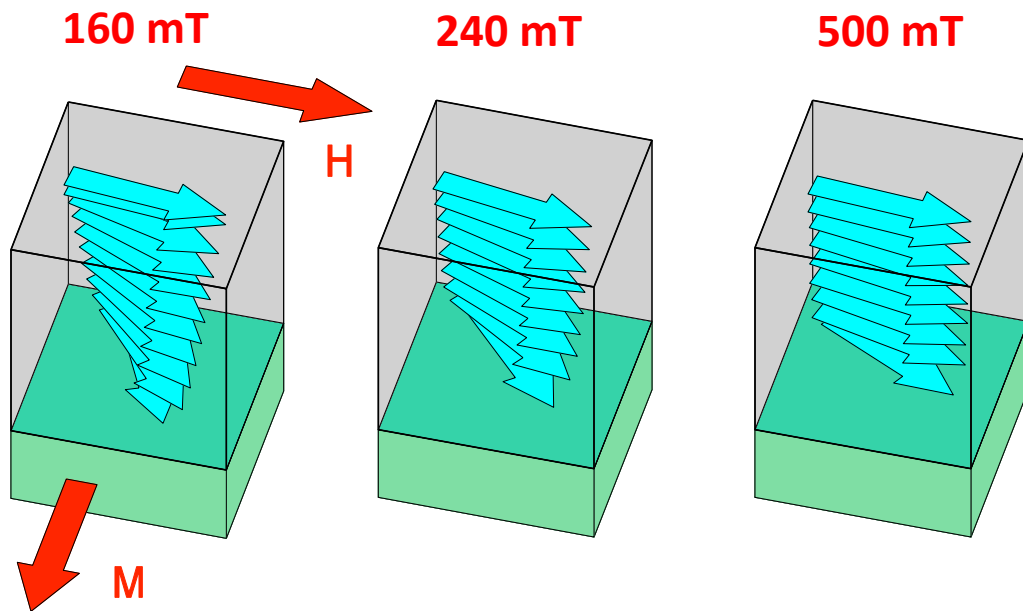


Imaging the Internal Spin Structure of Exchange-Spring Magnets

Time spectra of nuclear resonant scattering



**Domain wall
compression with
increasing external field**
Fe on FePt



Simulation of Exchange-Spring Layer Systems

E. Fullerton et al. PRB 58, 12193 (1998)

$$E = - \sum_{i=1}^{N-1} \frac{A_{i,i+1}}{d^2} \cos(\varphi_i - \varphi_{i+1})$$

Exchange

$$- \sum_{i=1}^N K_i \cos^2 \varphi_i$$

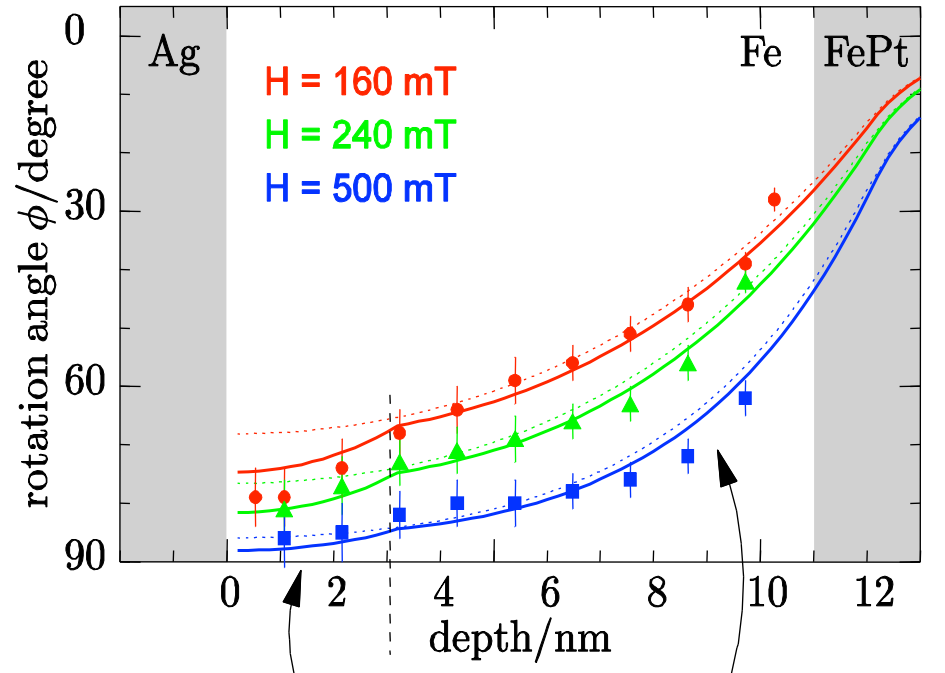
Anisotropy

$$- \sum_{i=1}^N H M_i \cos(\varphi_i - \varphi_H)$$

Dipolar energy

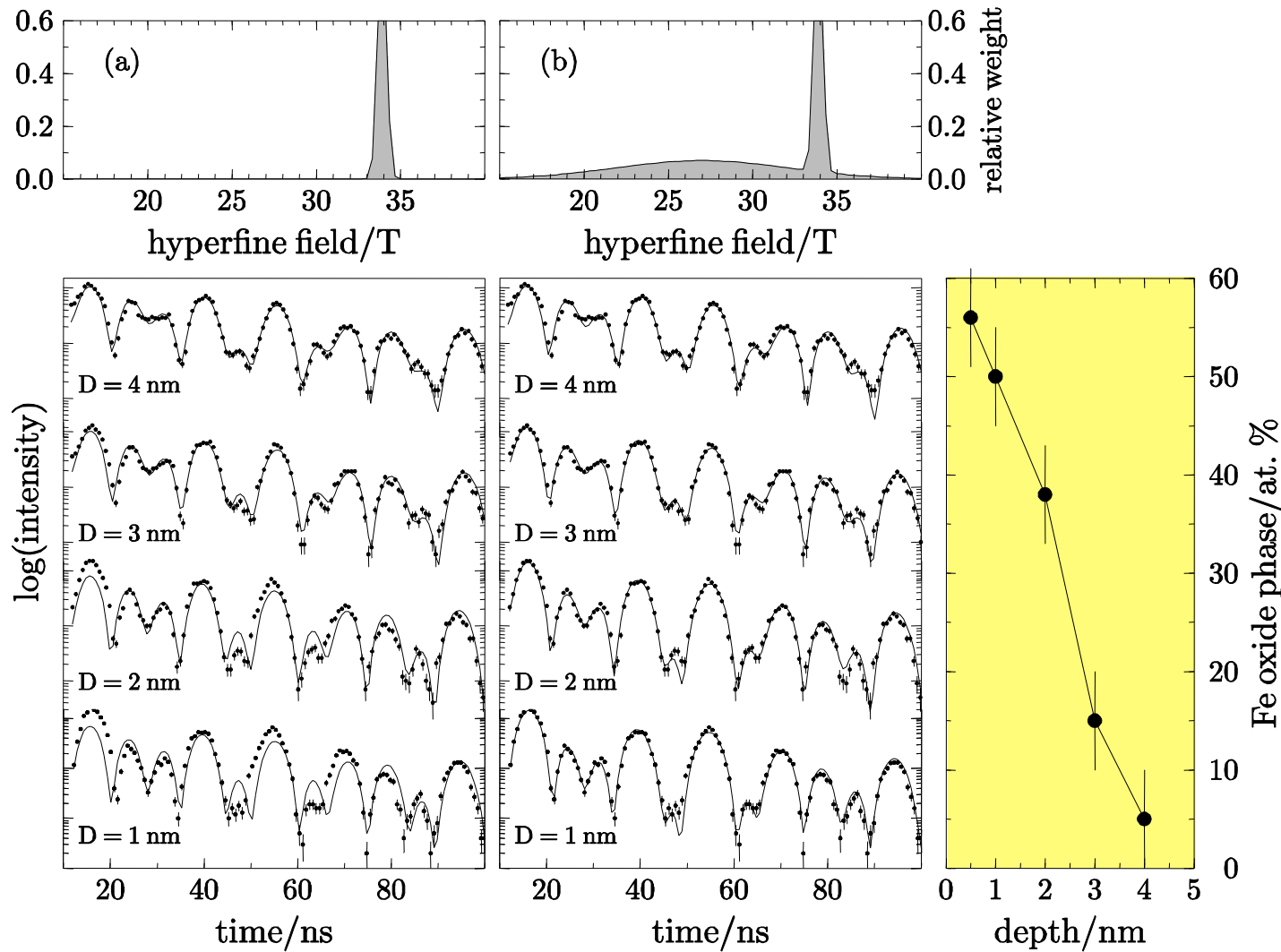
Divide the layer system into N sublayers of thickness d

Minimize the magnetic free energy $\frac{\partial E}{\partial \varphi_i} = 0$



Depth profiling of magnetic properties

Depth Dependence of the Oxide Phase

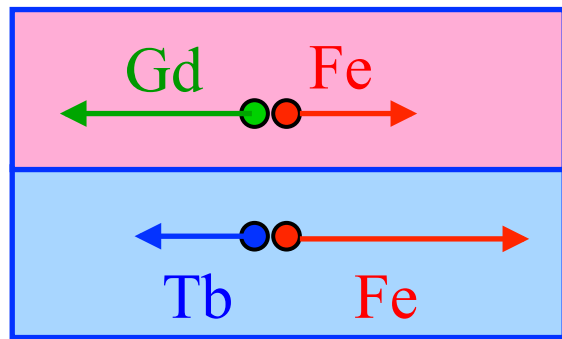


RR, H. Thomas, K. Schrage, T. Klein, J. Magn. Magn. Mater. 282, 329 (2004)

Exchange-Coupling of TbFe/GdFe Bilayers

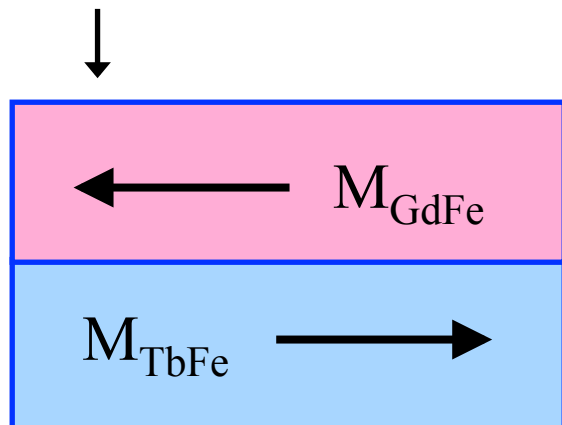
TbFe, GdFe → Amorphous alloys, produced by co-evaporation of the constituents at T = 77 K in an external field

Exchange constants: $|J_{\text{FeFe}}| > |J_{\text{FeGd}}| > |J_{\text{FeTb}}| > |J_{\text{GdTb}}|$



Gd₄₀Fe₆₀ Soft ferrimagnetic alloys

Tb₁₂Fe₈₈ Soft-magnetic at room temperature,
hard-magnetic at low temperature

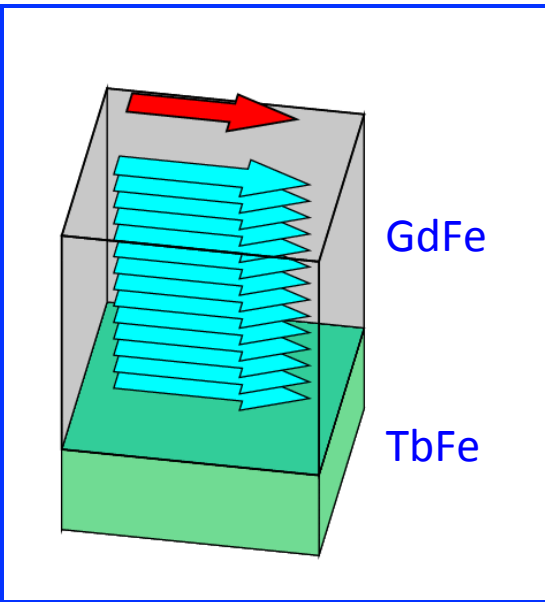


Adjusting the type of coupling via composition of the alloys

In collaboration with

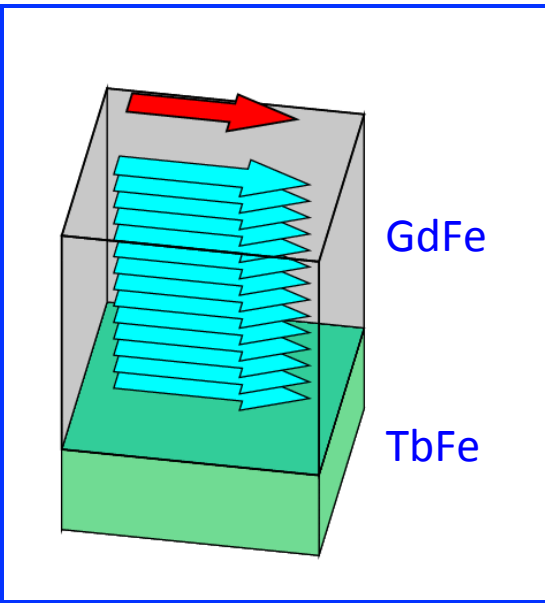
S. Mangin, F. Montaigne, T. Hauet (Nancy)
J. Juraszek, J. Teillet (Rouen)

Domain Wall Compression in FeGd/FeTb



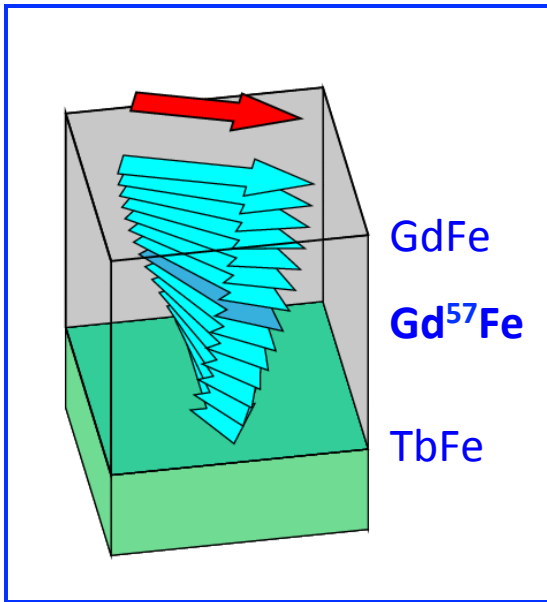
Cooling the sample in an external field below T_B freezes the spin configuration in the TbFe layer

Domain Wall Compression in FeGd/FeTb



Sample rotation in the field induces a twisted magnetic state (planar domain wall)

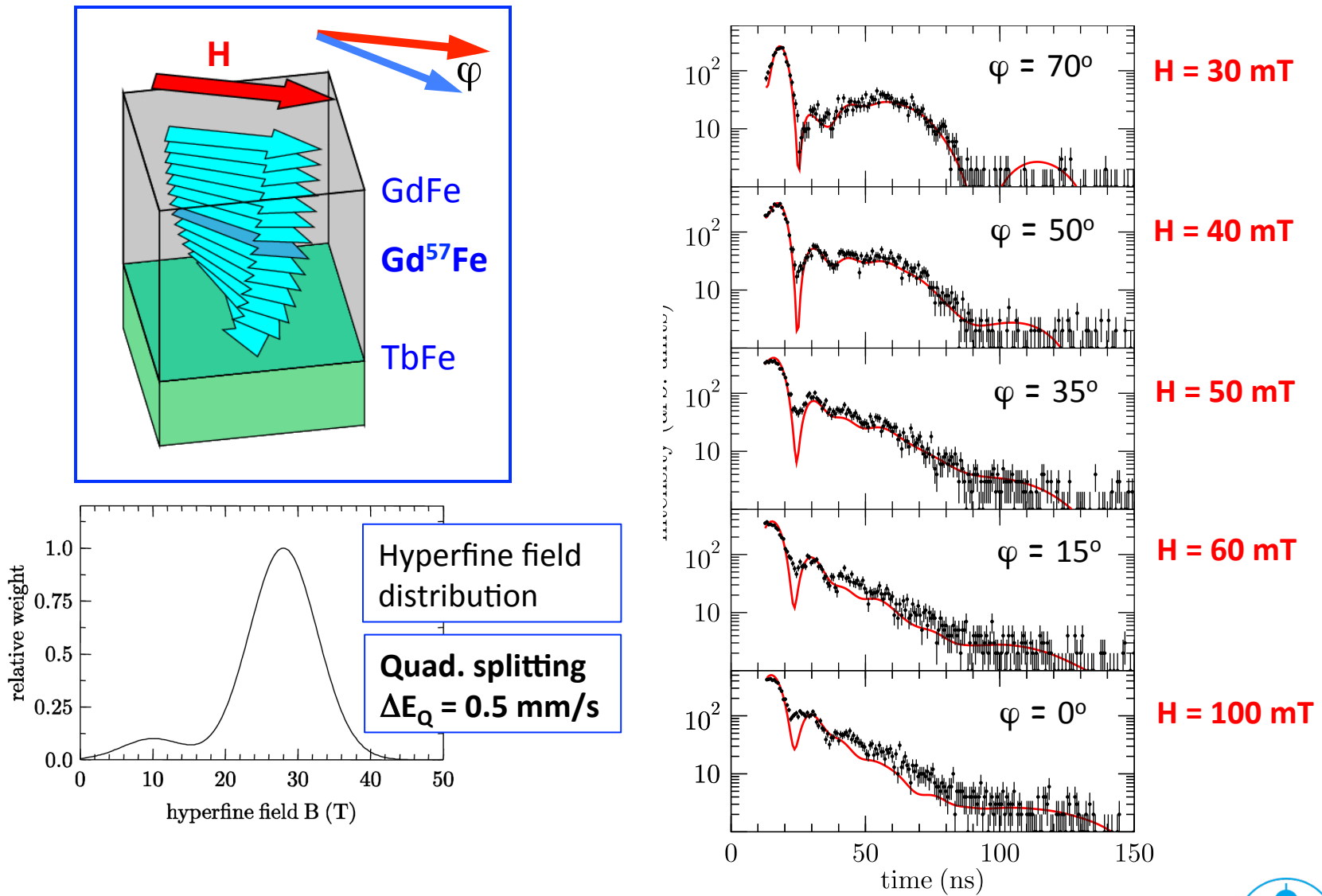
Domain Wall Compression in FeGd/FeTb



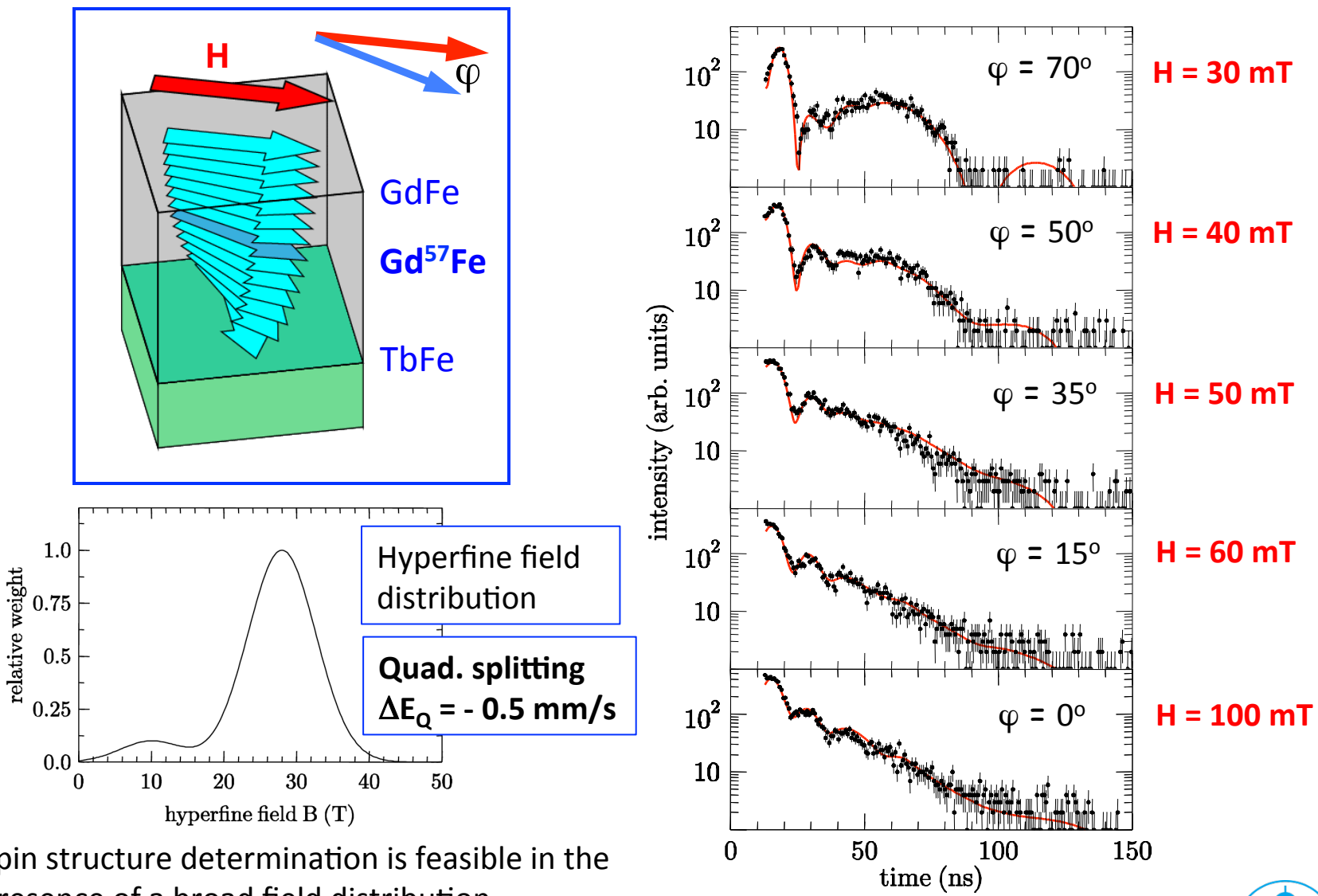
Increase of the external field leads to domain wall compression

Insert Gd⁵⁷Fe probe layer to observe the compression (**dark blue arrow**)

Domain Wall Compression in FeGd/FeTb



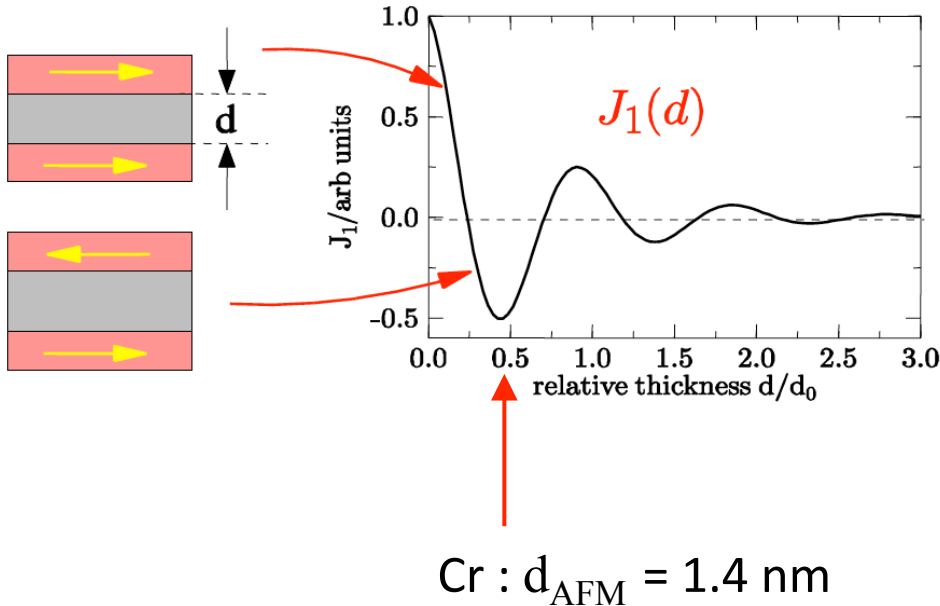
Domain Wall Compression in FeGd/FeTb



Spin structure determination is feasible in the presence of a broad field distribution

Magnetic Order in Fe/Cr multilayers

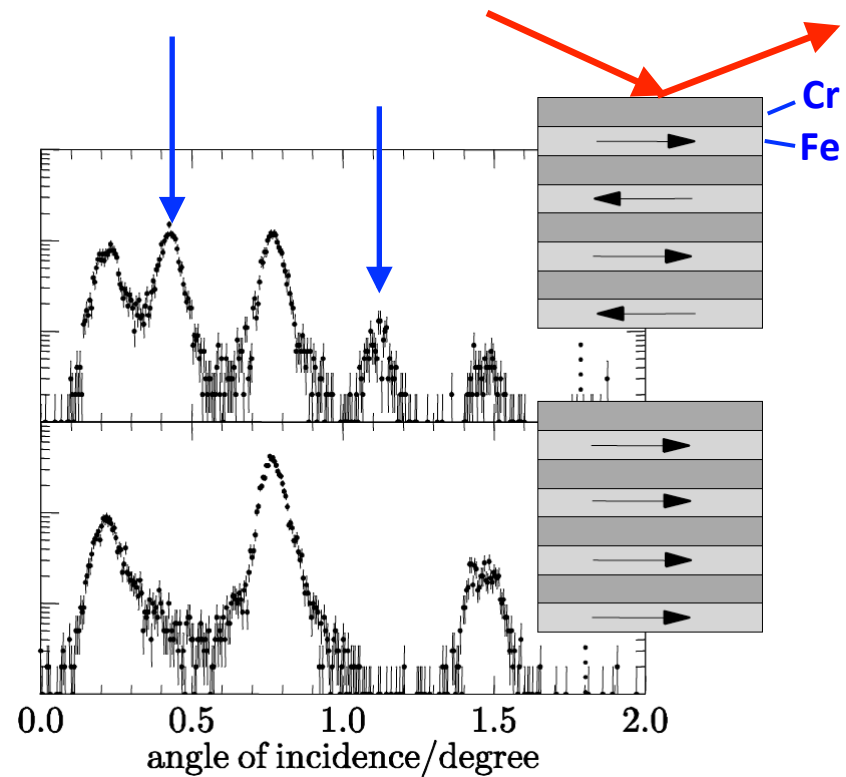
RKKY- oscillatory interlayer coupling



“There is no home like Iron-Chrome”

detected via nuclear resonant scattering of synchrotron radiation :

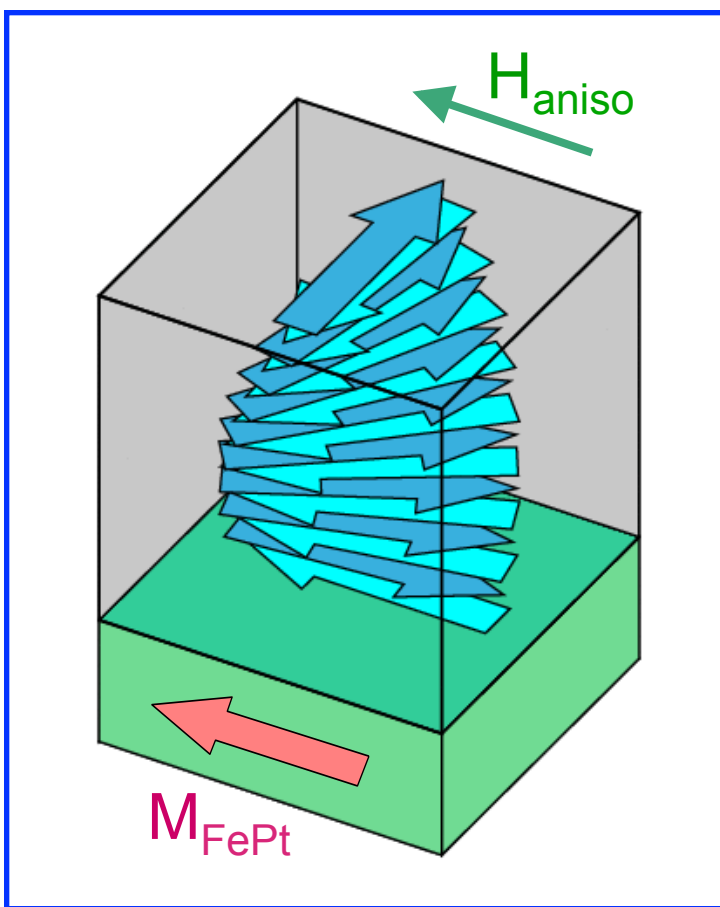
Half-order Bragg peaks due to magnetic superstructure



T. Toellner et al., PRL 74, 3475 (1995)

Twisted States in Exchange-Coupled Antiferromagnetic Multilayers

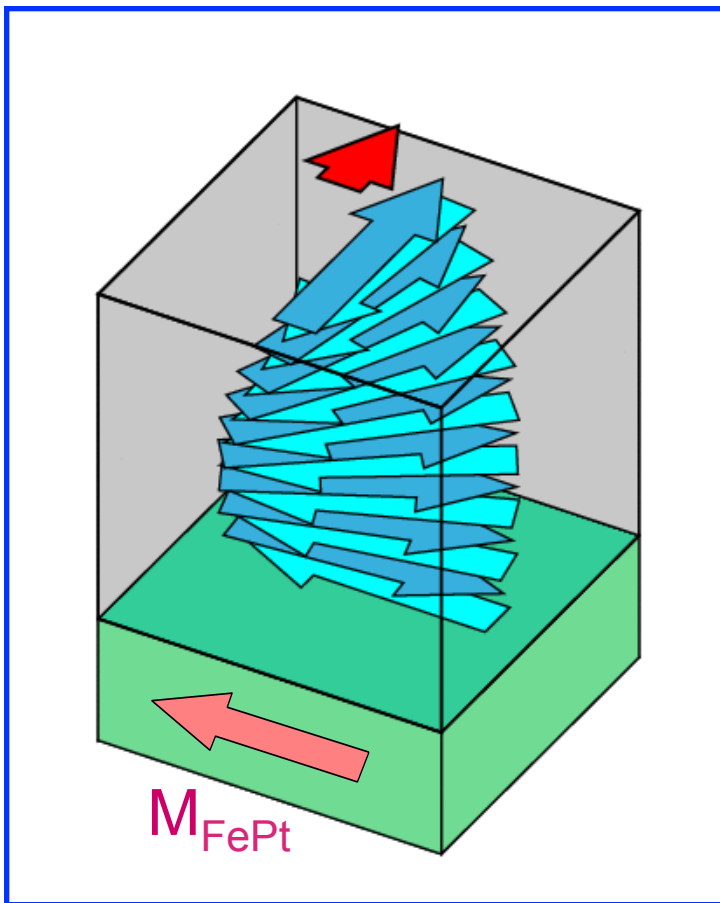
Fe/Cr multilayer exchange coupled to hard-magnetic FePt with unidirectional magnetic anisotropy



Twisted state stabilized by

- a) External field
- b) Intrinsic anisotropies, acting as an effective external field

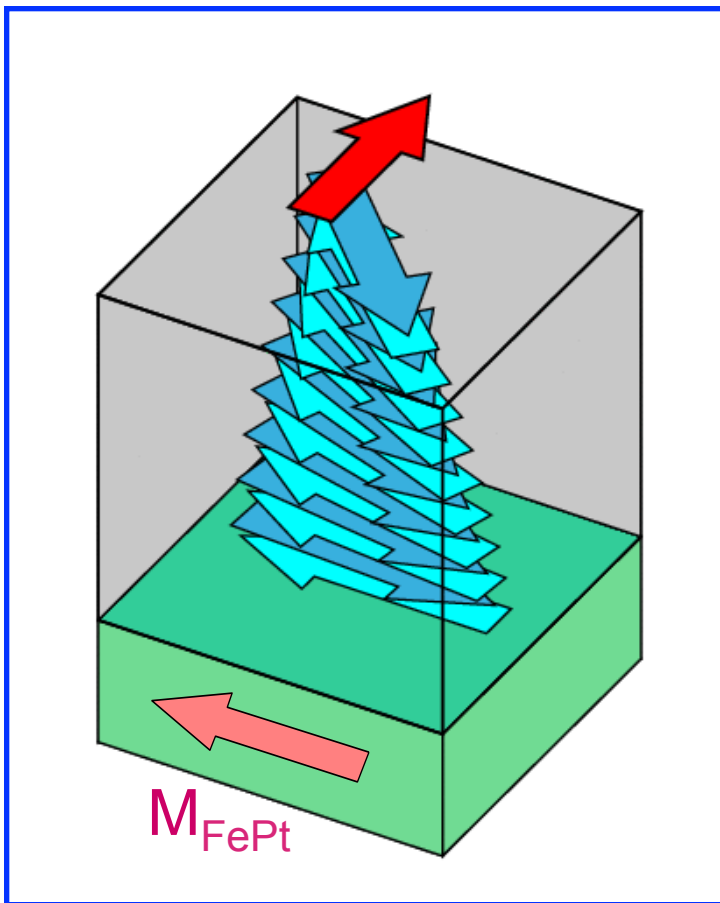
Twisted States in Exchange-Coupled Antiferromagnetic Multilayers



External field increases the twist angle

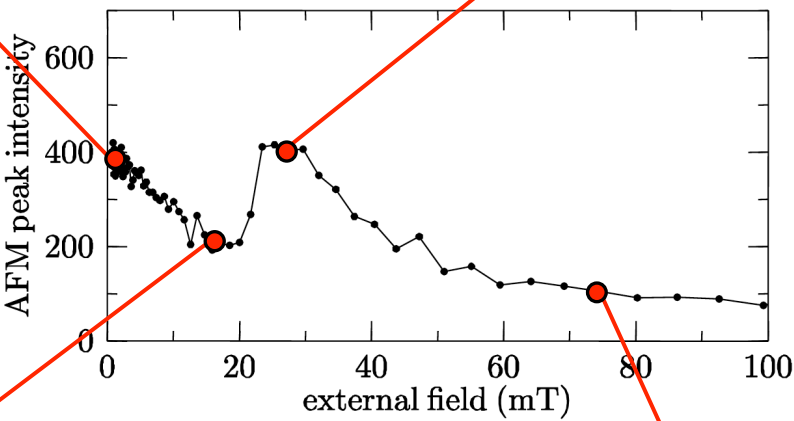
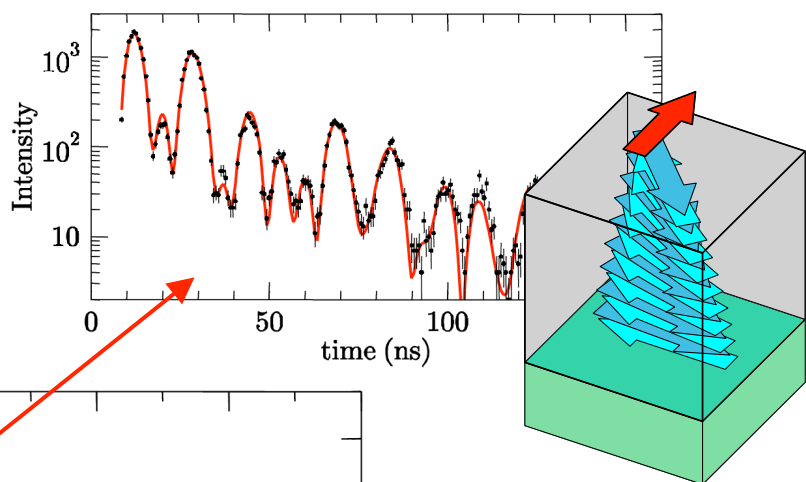
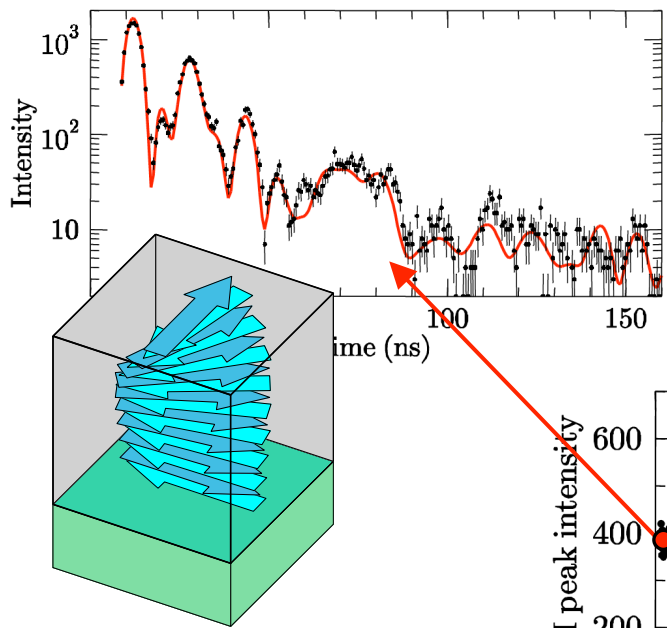
The potential energy of the magnetic spring increases

Twisted States in Exchange-Coupled Antiferromagnetic Multilayers

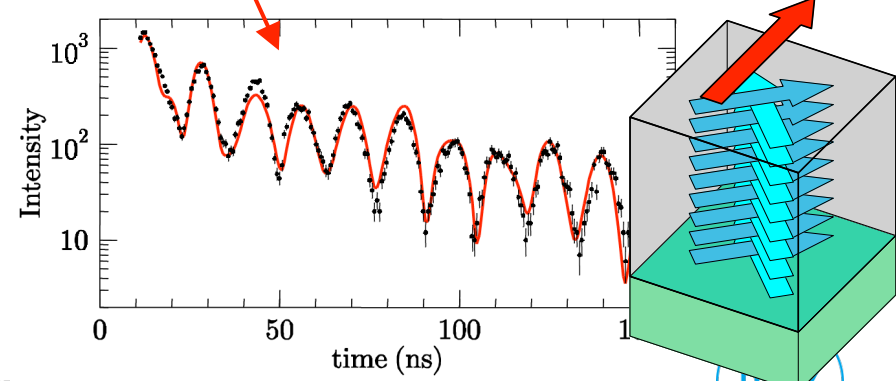
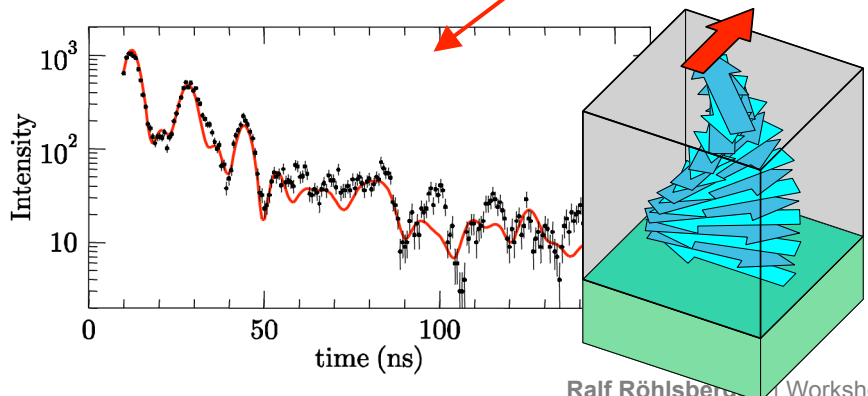


System moves into state of lower energy by changing its chirality

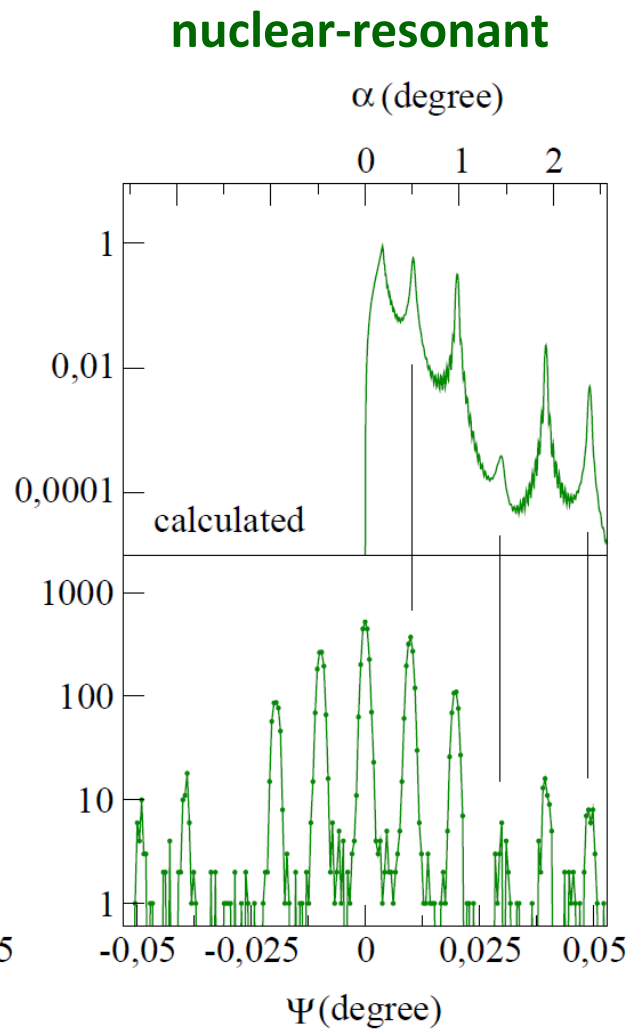
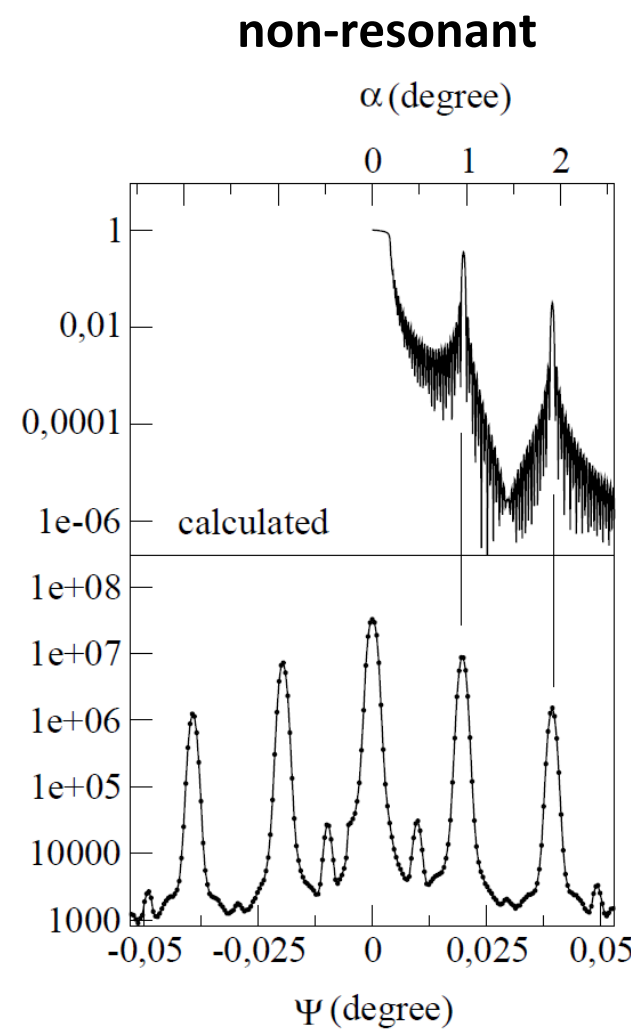
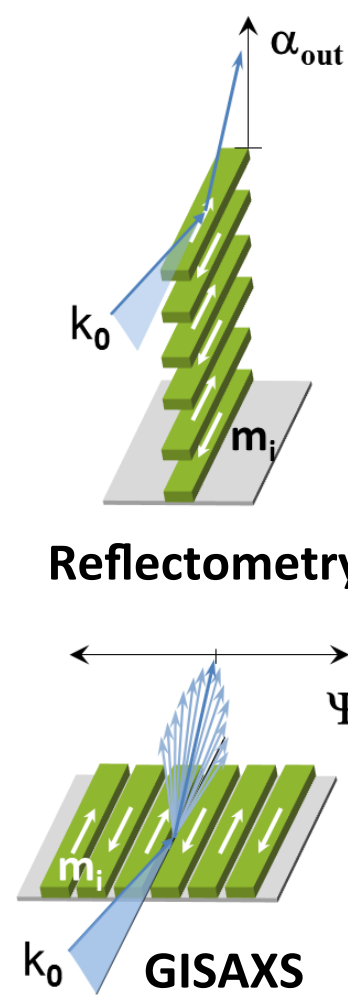
Observation of Chirality Reversal



K. Schrage et al. (2005)

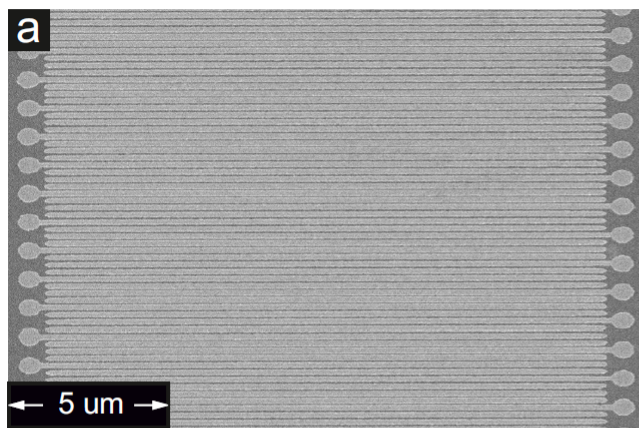


From vertical to horizontal (lateral) magnetic structures



Magnetic Superstructure in Arrays of Nano Wires

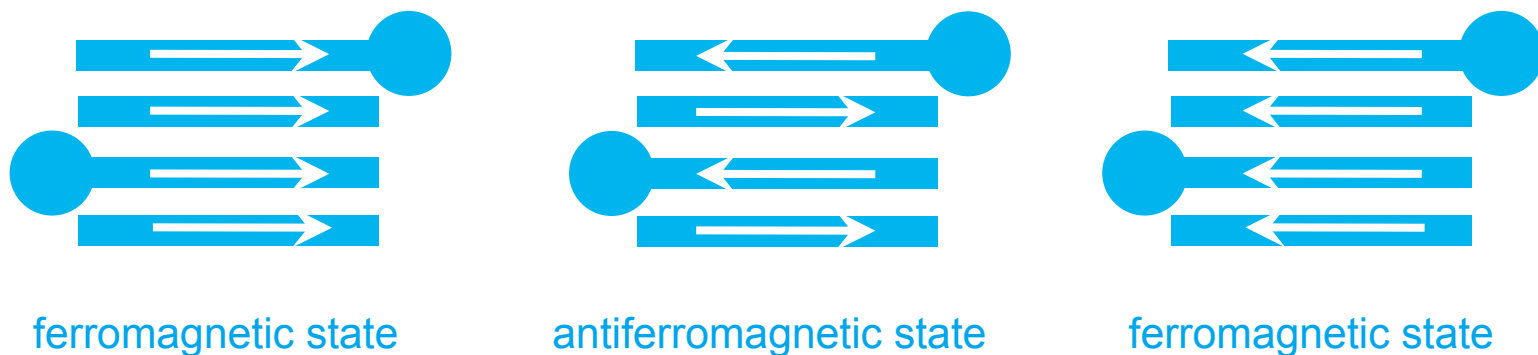
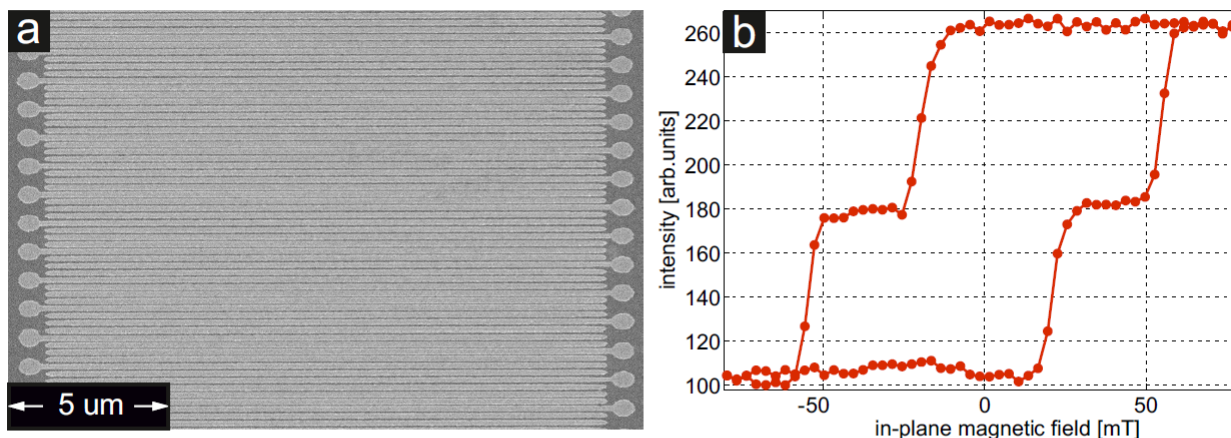
30 nm thick Permalloy ($\text{Ni}_{80}^{57}\text{Fe}_{20}$) nano stripes with pads prepared by electron beam lithography and lift off technique at the IAP (Liudmila Dzemiantsova, Lars Bocklage)



soft magnetic
hard magnetic
soft magnetic
hard magnetic

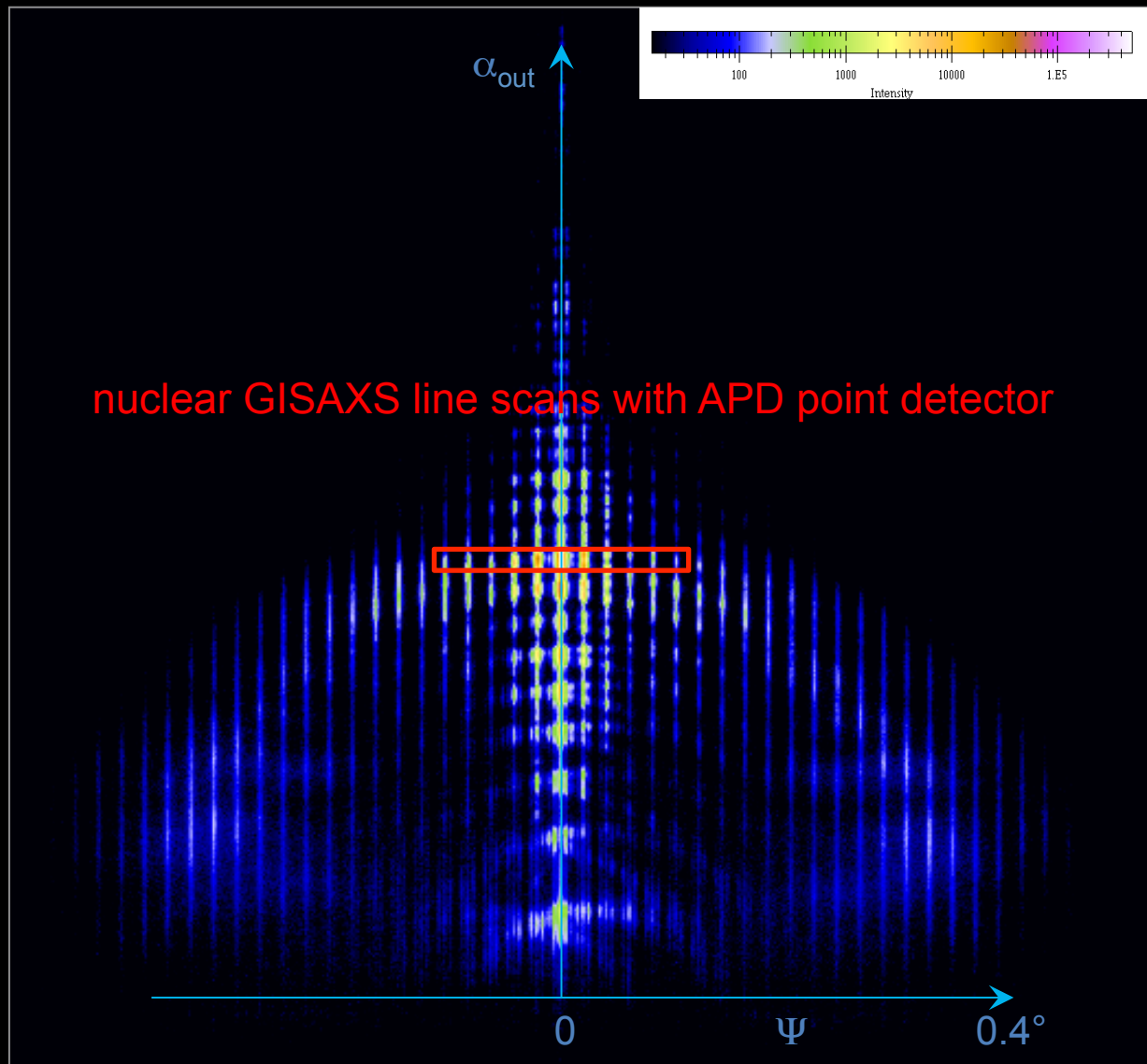
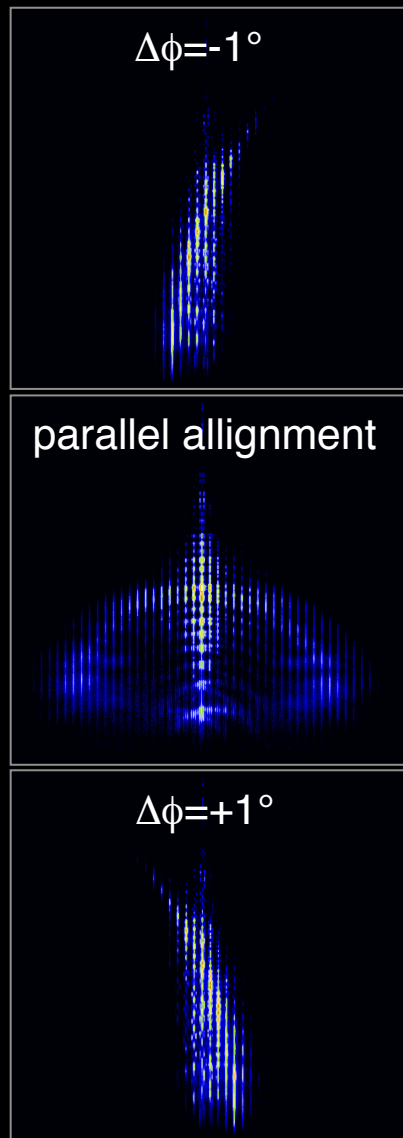
Magnetic Superstructure in Arrays of Nano Wires

30 nm thick Permalloy ($\text{Ni}_{80}^{57}\text{Fe}_{20}$) nano stripes with pads prepared by electron beam lithography and lift off technique at the IAP (Liudmila Dzemiantsova, Lars Bocklage)



- + successful preparation of perfectly antiparallel aligned nano stripes?!
- relatively large spacing of 500 nm in magnetic lattice, small sample

GISAXS on Permalloy Nano Stripes



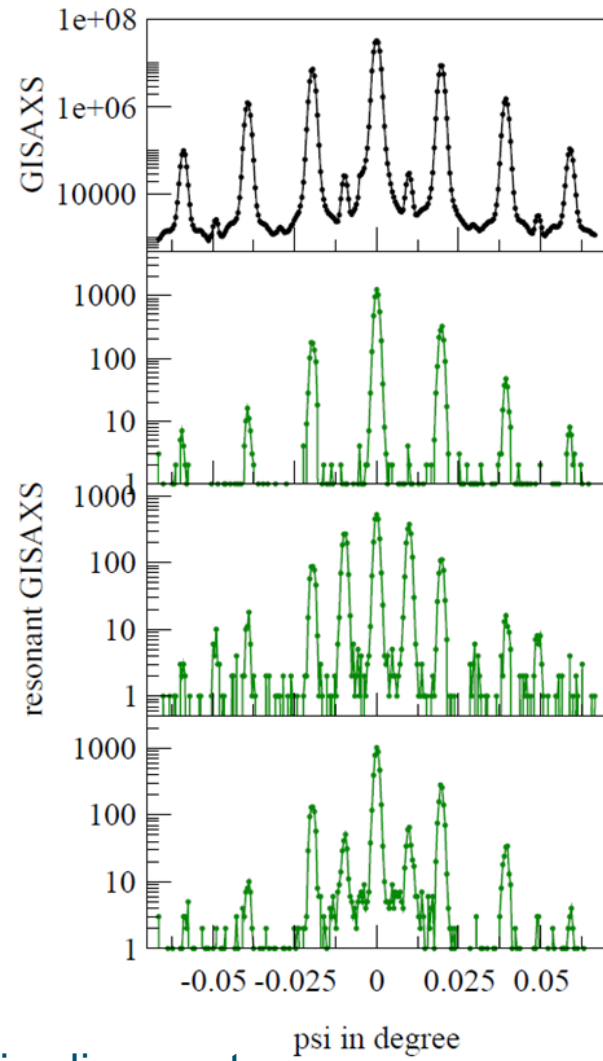
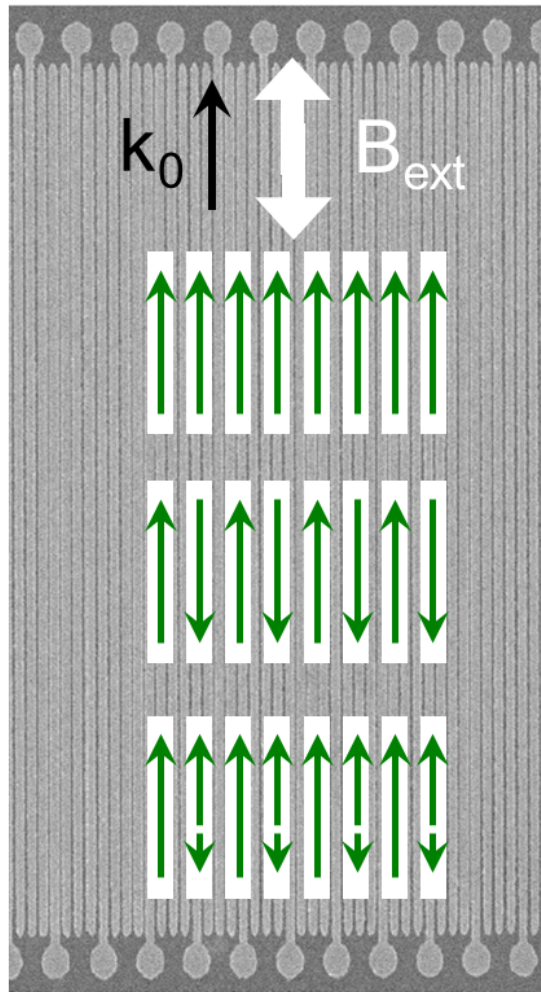
Resonant GISAXS on Permalloy Nano Stripes

magnetic states
of nano stripes:

ferromagnetic

antiferromagnetic

ferrimagnetic



Superstructure peaks indicate antiferromagnetic alignment.

Applicable to other periodic sample systems.

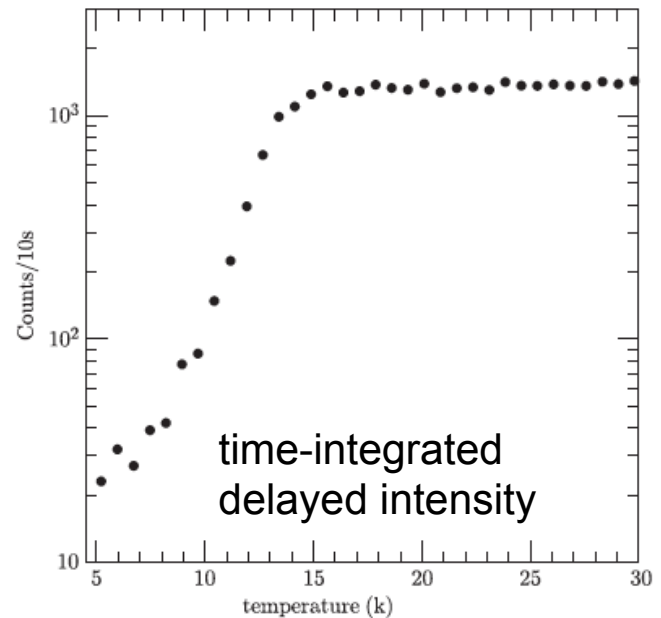
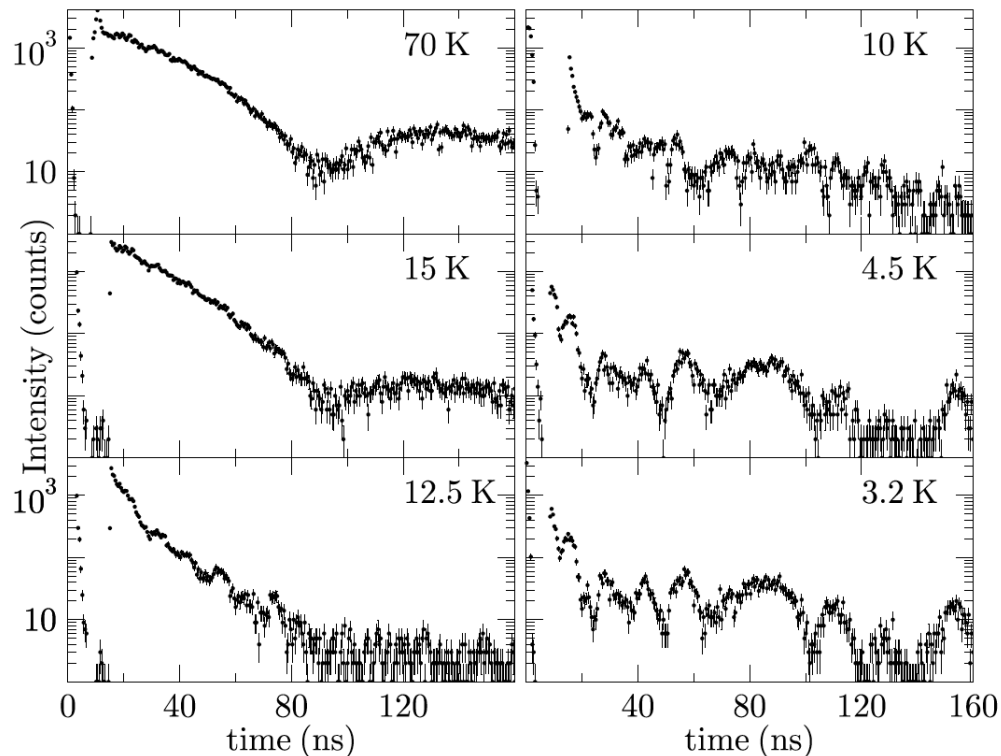
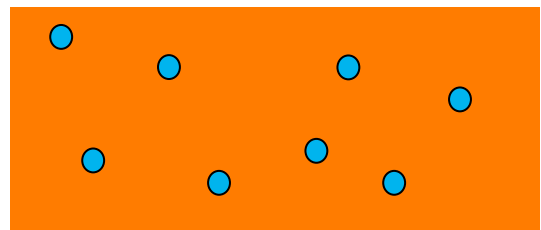
Determination of magnetic dynamics via nuclear resonant scattering

Probing Magnetic Relaxation: Fe₂O₃-oxide clusters in Cu

Magnetic moments are fluctuating with a rate much faster than $1/\tau_0$
sample appears nonmagnetic

$$\tau = \tau_0 \exp\left(\frac{KV}{k_B T}\right)$$

V = particle volume
K = anisotropy constant

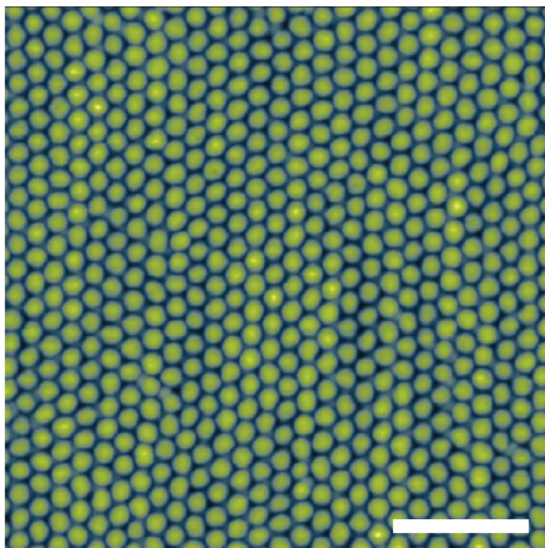


Magnetic moments are ‘frozen’
→ **sample appears magnetic**

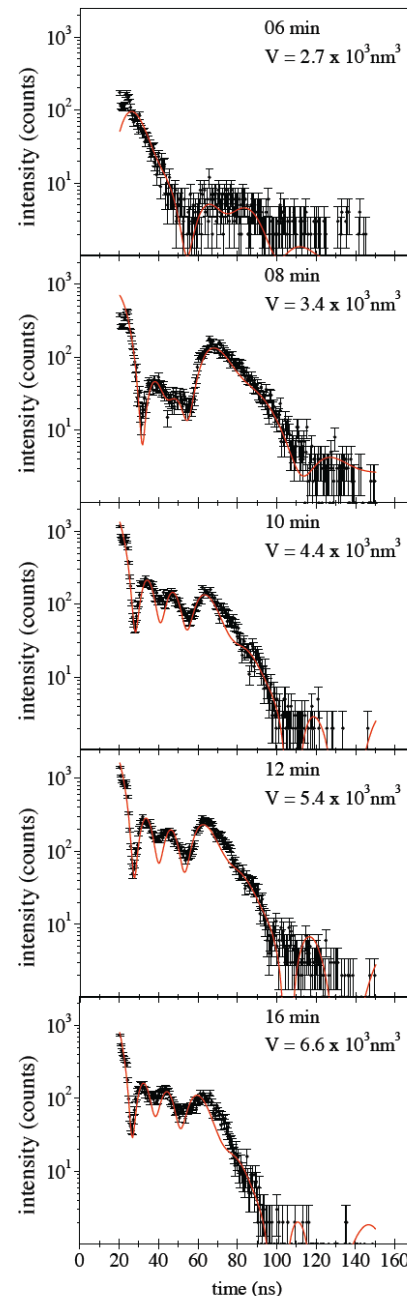
Magnetic Relaxation in Nanodots

Nuclear resonant scattering is very sensitive to magnetic dynamics

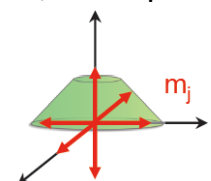
Fe nanoparticles on patterned diblock-copolymer films
(Ph.D. thesis of Denise Erb (2015))



$$f = f_0 \exp\left(-\frac{KV}{k_B T}\right) \quad V = \text{particle volume} \quad K = \text{anisotropy constant}$$

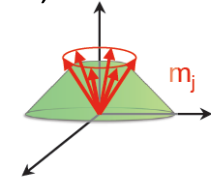


$f = 7.1 \text{ MHz, isotropic}$



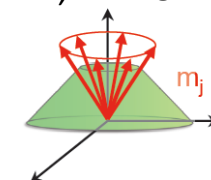
$f = 6.7 \text{ MHz, } \alpha = 32^\circ$

$f = 6.4 \text{ MHz, } \alpha = 32^\circ$



$f = 6.4 \text{ MHz, } \alpha = 32^\circ$

$f = 6.4 \text{ MHz, } \alpha = 28^\circ$



Nuclear Resonant Scattering for Magnonics

Magnetic resonances

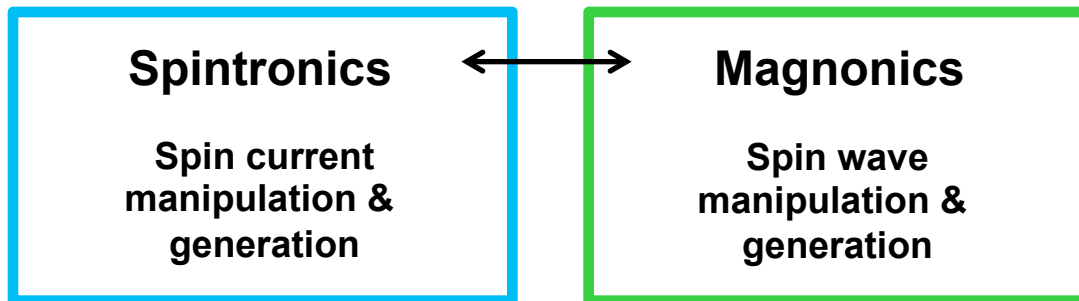
magnetic storage → switching times, energy losses



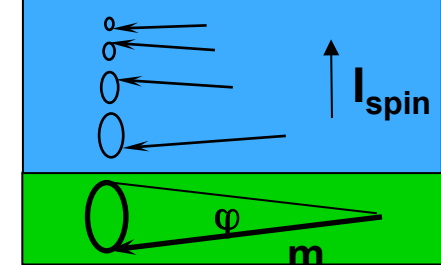
www.hitachigst.com

Spin manipulation

functional spin devices



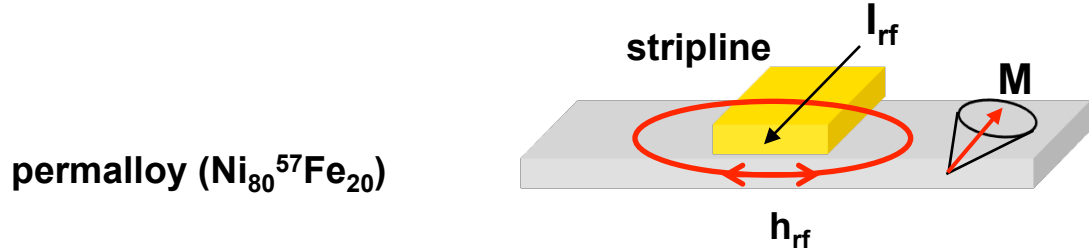
Spin Pumping



Y. Tserkovnyak et al. , Phys. Rev. Lett. 88, 117601 (2002)

Spin excitations in magnetic microstructures

Thin film system



permalloy ($\text{Ni}_{80}^{57}\text{Fe}_{20}$)

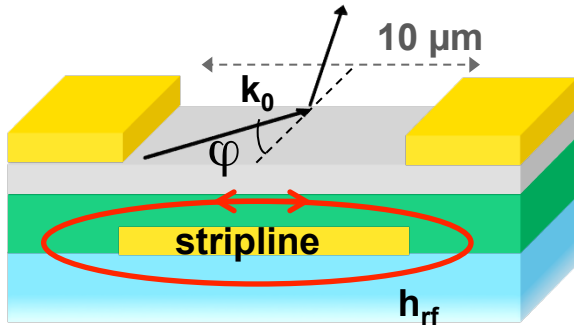
Goal: Excitation of uniform spin precession
→ Kittel mode at ferromagnetic resonance

Experimental Setup

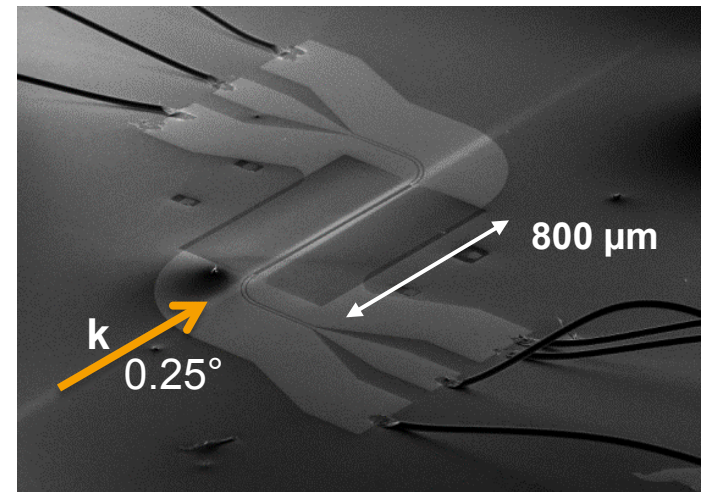
(CUI Project C3.2)

Thin film system

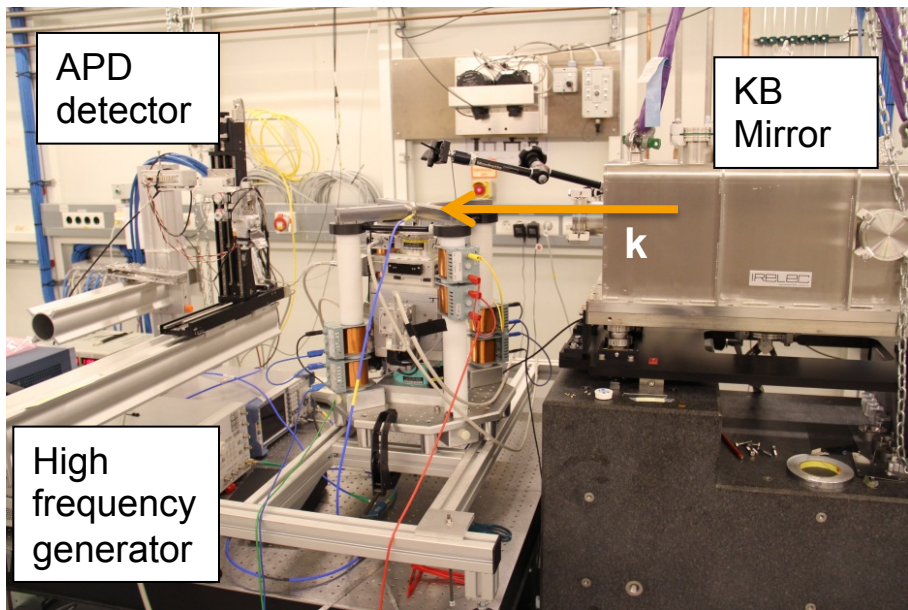
Au 30 nm
permalloy ($Ni_{80}^{57}Fe_{20}$) 13 nm
insulation (HSQ) 170 nm
GaAs substrate



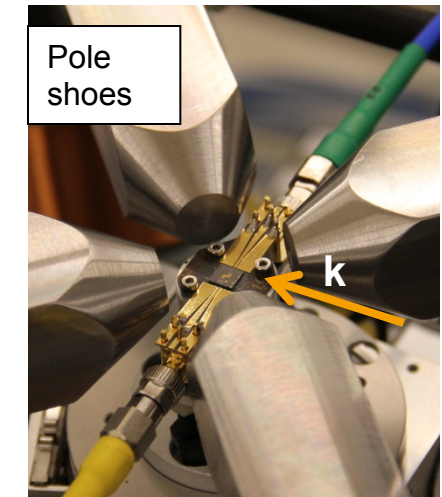
grazing incidence



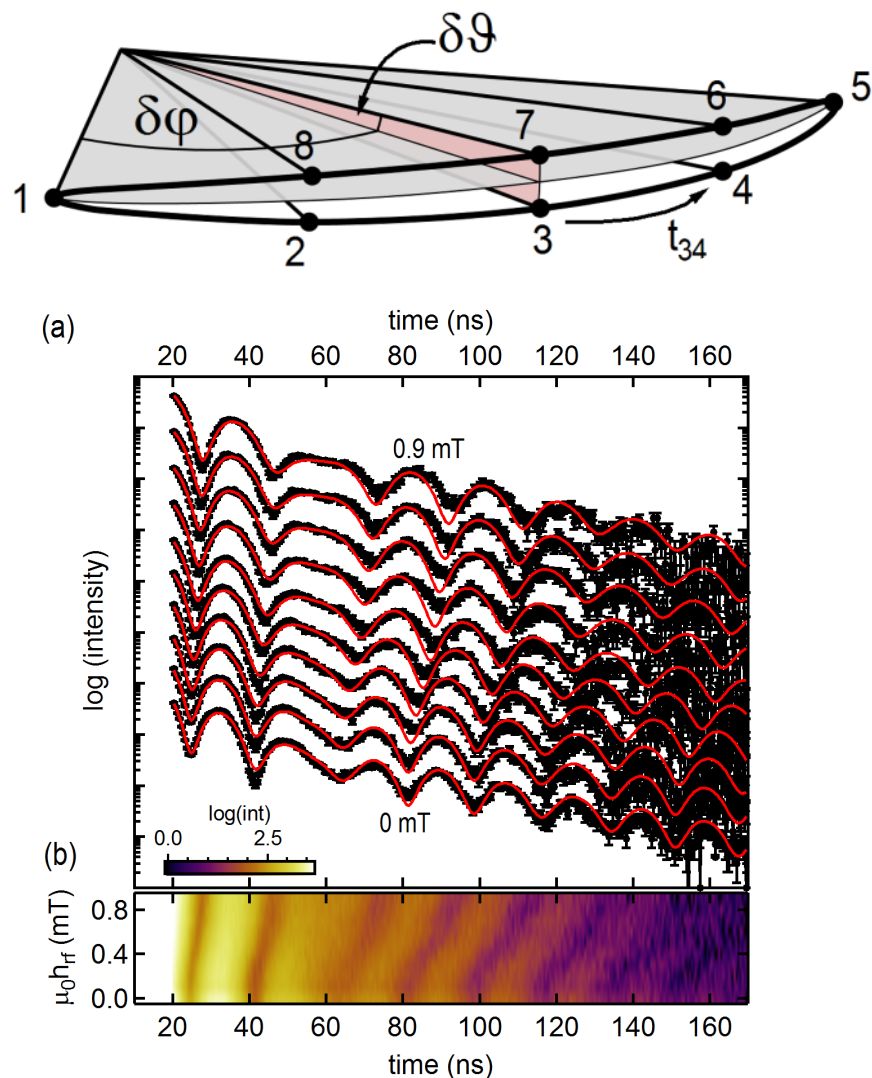
Setup at beamline P01 of PETRA III



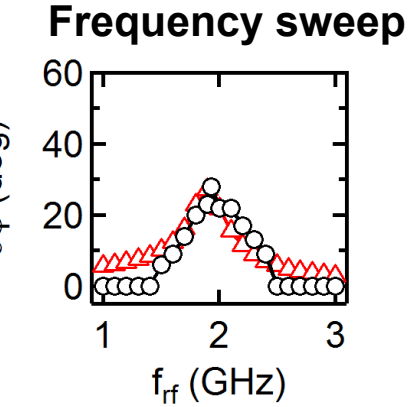
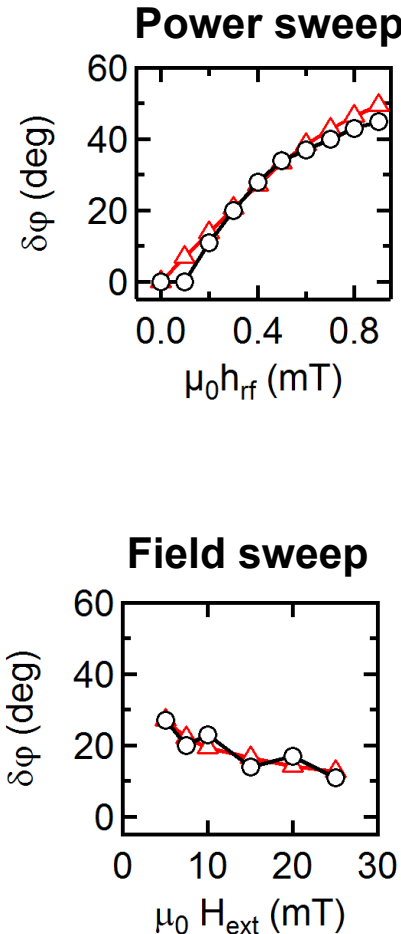
KB mirror focus
 $10 \times 10 \mu m^2$
matches typical sample size



Spin trajectory determination



Determination of the opening angle $\delta\varphi$

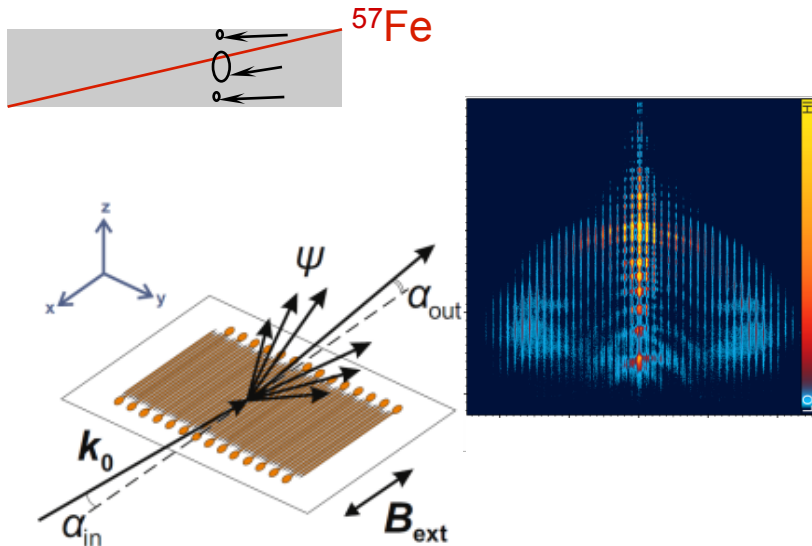
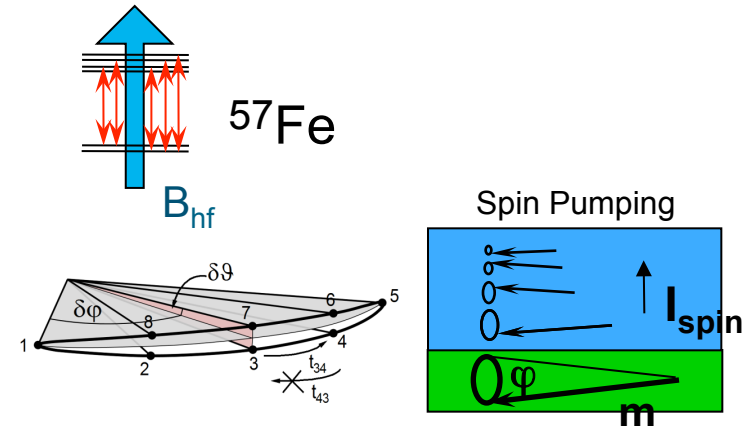


micromagnetic
simulations with
MicroMagnum
software

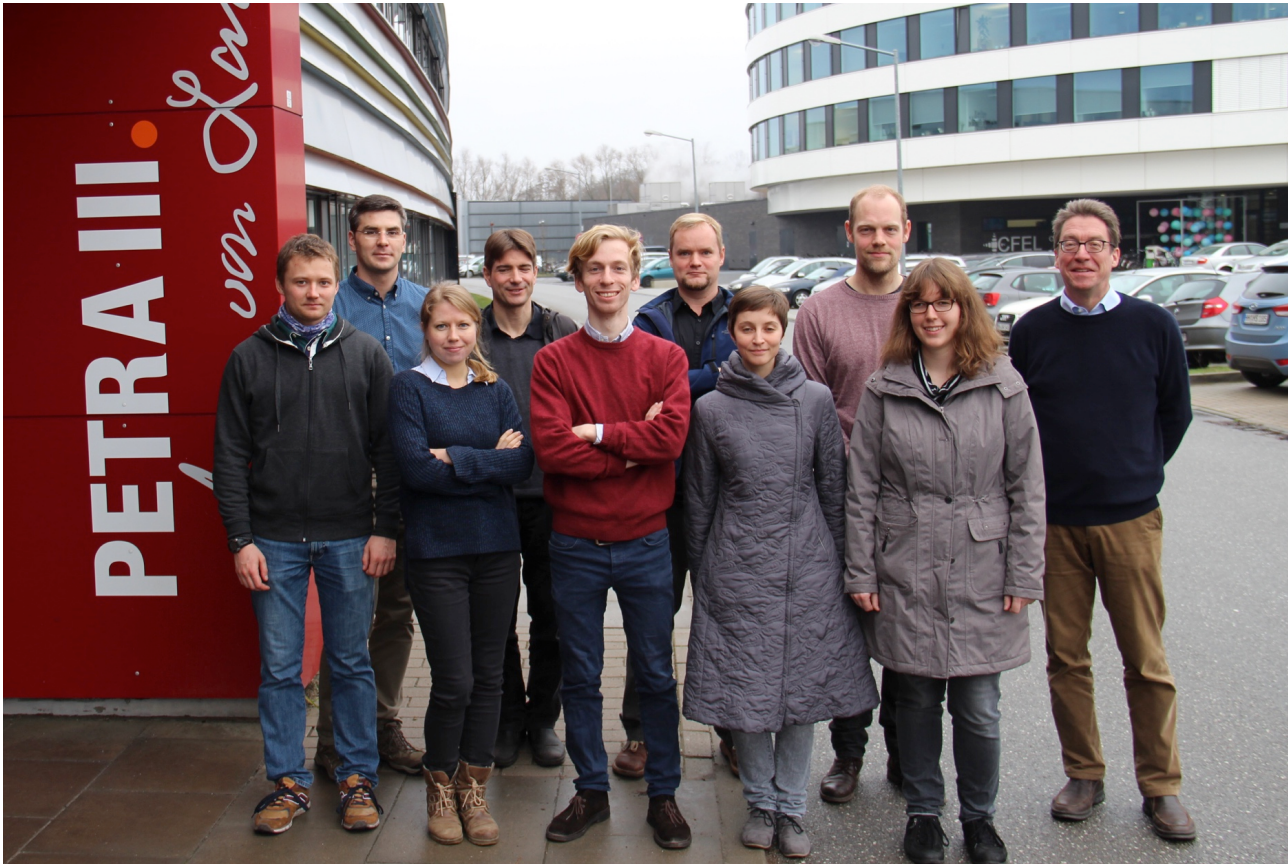
L. Bocklage et al., Phys. Rev. Lett. 114, 147601 (2015)

Summary

- Nuclear resonant scattering to study spin structure and spin dynamics
- Determination of magnetic relaxation rates and precession trajectories
- New approach to study magnetization dynamics
 - Depth profile of spin waves via thin isotopic probe layers
 - Non-equilibrium spin dynamics in strongly correlated systems



The Group ‘Magnetism and Coherent Phenomena’



Andrey Siemens

Pavel Alexeev **Liudmila Dzemiantsova**

Cornelius Strohm

Johann Haber

Kai Schlage

Lars Bocklage

Denise Erb **Svenja Willing**

not on picture: Jakob Gollwitzer